

Responses to Referee #1

”Surface roughness during depositional growth and sublimation of ice crystals” *by Cédric Chou et al.*

The authors describe a new laboratory setup for investigating roughness of single ice crystals grown in the apparatus. Their main result is the appearance of a ratcheting up of ice surface roughness/irregularity as crystals are subjected to cycles of growth and sublimation, a memory effect. Motivation for the work is given in terms of the radiative properties of ice-containing clouds in Earth's atmosphere.

I found this to be a useful and interesting contribution to what seems to be a still poorly constrained topic (ice surface roughness). The experimental apparatus and analysis methods seem to be described in sufficient detail, with a few minor exceptions (see below). The time-lapse videos provided in on-line supplement were especially valuable in aiding the interpretation of figures 10 and 11, but the manuscript stands on its own even without them.

We thank the Referee for the encouraging and insightful comments, questions and helpful suggestions. We list them below, together with our clarifications and changes to the manuscript in blue.

1. It seems that the discussion of whether ablation leads to more or less roughening should be improved in a couple of ways. Figures 10 and 11 do seem to suggest that ablation conditions tend to reduce roughness, but I think the videos of the 2-D scattering patterns tend to tell this story more clearly. And there are more interesting patterns evident in those videos: what are the bands caused by? Finally, while the literature references given by the authors seem to point in the opposite direction, it seems worth mentioning that at least one SEM study (Butterfield et al, Quantitative three-dimensional ice roughness from scanning electron microscopy, 2016) appears to support the authors findings that ablating crystals tend to be less rough.

We believe that most readers would find it hard to interpret the videos - that's why we rely on the quantitative measure of roughness instead. But to aid the interpretation, in addition to the existing explanation in section 3, we now provide further explanatory text at the end of section 2.3:

”The presence of isolated bright spots or bands is an indication of flat crystal facets, while spots covering a large proportion of the pattern signify the presence of roughness or high complexity”.

We have not cited the work of Butterfield et al. (2016) because in common with many other studies (several of which we do cite) it investigated ice growth in near vacuum, which as we argue is less relevant to atmospheric processes, and because it did not control for supersaturation, which we find to be a critical factor.

2. I found the discussion of roughening mechanisms more speculative than the authors let on. In particular, the last paragraph of section 3.1: none of what is presented in that paragraph is substantiated by evidence given in the paper. I also have a problem with the attribution at the beginning of section 3.1, in which the statement the growth rate is slow enough for the deposited molecule to diffuse on facets to well-separated attachment sites at steps, kinks, and ledges is not really justified, even if one can find such statements in the literature. I would point the authors to numerous studies that show that the picosecond-scale sticking coefficient on the quasi-liquid layer of ice is close to 1, and conversion of quasi-liquid to ice occurs faster than horizontal diffusion permits Neshyba et al, A quasi-liquid mediated continuum model of faceted ice dynamics, 2016, offer an alternative view. In general, I found it puzzling that there was no mention of the role of the quasi-liquid layer in these sections; if they are going to speculate, at least that factor ought to be included. At the very least, the authors should flag these sections as more highly speculative than currently indicated.

We admit that our discussion is speculative, not least because this initial study focuses mainly on quantifying the phenomenology, rather than the causes, so we have insufficient information at this stage to pinpoint definite origins of the observed roughness. Nevertheless, the Reviewer’s comment highlights the major issue we have already pointed out: different growth studies show differences in crystal behaviour that remain to be explained, and there are many, sometimes conflicting views reported in the literature. An attempt at clarification, also pointing out the difference between experiments in air and in near vacuum, was for example provided by an interactive comment in ACP by Kiselev (2014). To reinforce this last point we now insert additional text and references in section 3.2:

”This distinction is known to lead to different growth rates as well as habits (Beckmann, 1982; Kuroda and Gonda, 1984;”.

”Furthermore, in experiments carried out under atmospherically-relevant air pressures, crystals having undergone more than one growth cycle tended to develop more faults (Beckmann, 1982).”
and

”[A further difference between the diffusion limited and kinetics-limited growth is that the former can lead to] increased numbers of faults (Beckmann, 1982) and”

”Beckmann, W.: Interface kinetics of the growth and evaporation of ice single crystals from the vapour phase: III. Measurements under partial pressures of nitrogen, *J. Crystal Growth*, 58, 443451, doi:10.1016/0022-0248(82)90291-3, 1982.

Kuroda, T., and Gonda, T.: Rate determining processes of growth of ice crystals from the vapour phase, Part II: investigation of surface kinetic processes, *J. Meteor. Soc. Jap.*, 62, 563572, doi:10.2151/jmsj1965.62.3.563, 1984.”

For the atmospherically relevant case of growth and sublimation in air, we point out that the process is vapour diffusion limited, not limited by attachment kinetics. In this context, the timescale of the processes occurring on the surface is less critical, as more time is available for lateral diffusion. Moreover, the lateral diffusion lengths are reported to be high in this context (e.g. Pfalzgraf et al., 2011), justifying our qualitative description.

As for the relevance or otherwise of the quasi-liquid layer (QLL) concept itself, we have decided that this side topic was again too broad and complex to be discussed in our paper. Nevertheless, we can say here that while QLL appear to be important at warmer temperatures, close to the melting point, they become thinner and correspondingly less important at lower temperatures. At the temperatures relevant here the thickness of the QLL is reported to be very low, below the lattice constants of ice (e.g. Conde et al., 2008). We can also point out that much of this area is subject to a similar misapprehension as ice growth in vacuum: most QLL studies are done by molecular modelling in the absence of air, making them less relevant to atmospheric processes. This is compounded by differing use of terminology: molecular-scale roughness, much discussed in the literature, is different from the roughness on the ”optical” scale (i.e. on the scale of the wavelength of light or larger) that is the subject of this work. Moreover, to our knowledge, molecular dynamics modelling studies of the QLL have so far failed to replicate the surface roughness observed experimentally; it was even argued that roughness may arise due to processes at larger scale, potentially fitting the

stacking disorder connection postulated here (Pfalzgraf et al., 2010). On a broader note, we think that it would be brave to try to overturn decades of evidence and crystal growth theory by claiming overriding importance for QLLs in this context. They do not yet explain many features of ice surface growth (e.g. growth inhibition and supersaturation thresholds). Conversely, some relevant features can be explained, somewhat counter-intuitively, by layered growth without the recourse to QLLs, e.g. rounding during sublimation (Nelson, 1998). Layered growth and sublimation, and the presence of well-defined elementary steps and terraces has been demonstrated in many systems, including ice; moreover, it can lead to larger step heights (relevant here) through step bunching (e.g. Nelson, 1998; Peterson et al., 2010; Sazaki et al., 2010; Misbah et al., 2010). So we are unsure what the relevance of QLLs is and how to bring this concept in without making the discussion more speculative (which the Reviewer advises against).

Lastly, the Neshyba et al. (2016) study authors admit that the modelling conditions do not make it directly applicable to atmospheric processes (p. 14049 therein) and do not even refer to roughness; we therefore fail to see its relevance.

To clarify the importance of step growth, we insert the following text and additional references in section 3.2.

”Moreover, the bunching of elementary molecular steps, possibly due to the Schwoebel effect (Misbah et al., 2010), can result in the creation of larger, microscopic (as opposed to elementary) steps that can be seen in SEM micrographs (Cross, 1969).

Misbah, C., Pierre-Louis, O., and Saito, Y.: Crystal surfaces in and out of equilibrium: A modern view, *Rev. Mod. Phys.*, 82, 981-1040, doi:10.1103/RevModPhys.82.981, 2010.”

3. Mentions of diffusion-limited and attachment kinetics are unlikely to be understood by many ACP readers; I’d suggest elaborating a little, or omitting these points of discussion.

At the first mention we now additionally clarify that we refer to vapour diffusion. The distinction we point out is important, as it permits an evaluation of the (ir)relevance of various laboratory experiments to the atmospheric context, and differences between their outcomes. We have already provided several relevant references to kinetics- and diffusion-limited growth at several points in the article for interested readers to follow.

”...growth in the absence of air that takes place in a SEM chamber, instead of being limited by vapour diffusion as is the case for ice at tropospheric pressures, becomes limited by the attachment kinetics...”

4. I think it would be appropriate to point the reader to the authors own prior discussion of the possibility of roughness ratcheting-up, as in Ulanowski et al, 2014.

At the beginning of section 3.2 we now refer the readers to the prior discussion in the reference suggested.

”Ulanowski et al., 2014”

5. Some very minor points: I think the paragraph just preceding section 3.1 is misplaced; it seems to refer to figure 8, but that figure has not been introduced yet. In section 3.2, where reference is made to small scale vertical motions as a possible mechanism for formation of irregular crystals, it might help to clarify that those are (I presume) atmospheric vertical motions. And there are a few misspellings here and there (closeer” in section 3.1) that I presume will be weeded out in the next round of editing.

We have placed this explanatory text where it is because it refers to several subsequent figures. Concerning vertical motions, we insert the word ”atmospheric” for clarification.

References for Reply:

Conde, M. M., Vega, C., and Patrykiewicz, A.: The thickness of a liquid layer on the free surface of ice as obtained from computer simulation, *J. Chem. Phys.*, 129, 014702, doi:10.1063/1.2940195, 2008.

Kiselev, A.: Interactive comment on ”Mesoscopic surface roughness of ice crystals pervasive across a wide range of ice crystal conditions” by N. B. Magee et al., *Atmos. Chem. Phys. Discuss.*, 14, C4758-C4763, <http://www.atmos-chem-phys-discuss.net/14/C4758/2014>, 2014.

Sazaki, G., Zepeda, S., Nakatsubo, S., Yokoyama, E., and Furukawa, Y.: Elementary steps at the surface of ice crystals visualized by advanced optical microscopy, *Proc. Nat. Acad. Sci.*, 107, 19702-19707, doi:10.1073/pnas.1008866107, 2010.

Peterson, H., Bailey, M., and Hallett, J.: Ice particle growth under condi-

tions of the upper troposphere, *Atm. Res.*, 97, 446-449, doi:10.1016/j.atmos
res.2010.05.013, 2010.

Responses to Referee #2

”Surface roughness during depositional growth and sublimation of ice crystals” *by Cédric Chou et al.*

The manuscript Surface roughness during depositional growth and sublimation of ice crystals by Cedric Chou et al. describes a study of ice crystal growth and sublimation performed in a new experimental setup. The experimental apparatus uses a unique combination of devices (flow diffusion tube and 2D scattering instrument) thus assuring a novelty of the results. The study is also well planned and the setup is thoroughly characterized, both by CFD modeling and experimentally. The authors demonstrate a high level of understanding of the physics behind the experiment, even if the thermodynamic parameters of the experimental system are not fully controlled. The paper is definitely worth being published, but must be thoroughly revised in many respects. I wish the paper were written more clearly. Some sections, as addressed below, require thorough editing. The relationship between the crystal evolution and its morphological complexity is, however, convincingly demonstrated. This work should trigger off studies of this phenomena with a better control of the supersaturation and optical control of the crystal morphology. I would, however, avoid naming the effect discussed in this manuscript the surface roughness, because this implies a quite narrow range of texture features. The sublimation and regrowth of ice crystals often create a polycrystalline aggregate of tiny crystals that can have smooth surfaces. The ultimate example is the Bucky ball crystals as in Baran (2012). Should such aggregate be named rough or irregular or somehow else? Would scattering patterns on such crystals be identical? I would really like to see a thorough discussion of these issues in the introduction and a clear separation of surface roughness from the morphological irregularity throughout the manuscript. In some sense, this is already done by introducing the combined roughness based on the 2D scattering patterns analysis. The same should be done with respect to surface texture and geometry of the crystals, and the approach suggested in this manuscript (combination of microscope observation with scattering measurements) seems to be very promising for achieving this goal. Below please find my comments which I hope would be helpful in improving the readability of the manuscript. The parts in the

manuscript I am addressing are identified by page and line number and the citation are given in italic.

We thank the Referee for a very thorough and encouraging review and many insightful comments, questions and helpful suggestions that allowed us to improve the manuscript. We list them below, together with our clarifications (in blue) and changes to the manuscript.

1. Introduction: How is the surface roughness defined and what is the quantitative measure of surface roughness? In the introductory part, the irregularity of ice crystals seems to be treated in parallel with the concept of surface roughness. However, the manuscript is titled clearly surface roughness... . The introduction (and the manuscript) would very much benefit from a clear definition of surface roughness as compared to habit irregularity. It would be also very helpful if you could think of a way to introduce a quantitative parameter to characterize physical surface roughness.

We state clearly that fine surface roughness and large-scale irregularity are treated together. Further discussion of the meaning and significance of the measure of roughness goes beyond the scope of present work and is dealt with in detail in the cited articles (Ulanowski et al., 2012, 2014). Among others, it was pointed out that the lack of distinction between "roughness" and "complexity" from the point of view of 2-D scattering is likely to also apply to other light scattering properties. So the distinction may be to some degree artificial. Nevertheless, crystals in the experiments were relatively simple prisms, not complex ones, so the study is more directly relevant to surface roughness, hence our choice of emphasis.

2. Page 2 Line 31: In the experiments, the ice crystals are fixed within the measuring volume and exposed to thermodynamic conditions... were there many crystals in the sample volume?

We insert the text ", generally single,":

"In the experiments, the ice crystals, generally single, are fixed within the measuring volume and exposed to thermodynamic conditions simulating single or multiple growth cycles at various temperature and saturation ratio."

3. Page 3, line 24. ...which ensures that the 22? halo scattering from ice prisms is included. I am afraid a typical reader would not know what you are talking about. You cant expect anyone being familiar with refraction theory

in hexagonal ice columns. Is this detail really needed here? The same line, replace lower angles with smaller angles.

We alter the text to say "bright feature associated with the familiar halo occurring for ice prisms at the scattering angle of 22° ". We do replace "lower angles with "smaller angles", as suggested.

4. Page 3, line 25. The camera images are digitized as 12-bit TIFF files... you can't possibly mean that the camera produces analog images that have to be digitized afterward?

That is indeed what happens internally to the camera.

5. Page 3, line 30. Figure 2 does not show the fiber-optics illumination, could you show how it was located with respect to the sample volume?

The text mentions the illumination; we now add that it is "in-line" with the microscope tube and add extra detail in Fig. 2.

6. Page 4. Section 2.1.3 Operating principle. The content of this section does not correspond to its title. Is that the operation principle of the whole setup or the flow diffusion channel? Before describing the simulation results, please explain exactly what has been simulated and what was the purpose of the simulation (I presume, the fast control of water-ice supersaturation in the vicinity of ice crystal located in LISA).

We create instead a new section entitled "Numerical simulations and thermodynamic characterisation". Our statement concerning the purpose of the simulations was probably too short. We change the text substantially as given below. The purpose of the steady state simulations was not to show the fast control of water-ice supersaturation. For that a transient model would be required. The response time of the system was a) calculated from mass flow rates and total volume of the system, and b) measured.

"The thermodynamic conditions at the tube outlet were extensively studied by means of computational fluid dynamics (CFD) simulations of the laminar flow tube, and by measurements of flow velocity, temperature and dew point at the tube outlet. Both the numerical simulations and the measurements have been done to characterise the experimental setup, as well as to demonstrate the fast control of temperature and supersaturation in the measuring volume.

The numerical simulations were done with the commercially available CFD code Fluent (Ansys Inc., USA). The Fluent model is a general purpose FVM (finite volume method) CFD model allowing the simulation of a wide range of small scale fluid flow problems. Here, the flow through the flow tube was simulated including a multicomponent treatment of the flow. The model accounts for the coupled processes of mass and heat transfer. With respect to the geometry and the laminar flow regime, the simulations were done on a 2-dimensional axisymmetric Cartesian grid by means of a pressure based steady state solver. Additional information about the numerical model, which has already been successfully applied to the characterisation of the laminar flow tube LACIS, can be found for example in Stratmann et al. (2004); Voigtländer et al. (2004); Voigtländer (2007) and Hartmann et al. (2011).

To illustrate the operating principle of the laminar flow diffusion channel, calculated thermodynamic profiles along the tube axis are shown in Fig. 3. ...”

7. Some sentences don't make sense to me: For a sufficiently high gas flow representing the residence time of the gas flow, the thermodynamic equilibrium between the wall and the gas flow will not be reached. Does the flow represent the residence time or vice versa? Please rewrite in a clear language.

We modify the paragraph by adding the text:

”If the residence time of the gas flow (controlled by the mass flow rate) is large enough, the gas flow cools down until thermodynamic equilibrium with the tube wall is reached. Conversely, for a sufficiently fast flow equilibrium will not be reached.”

8. In Figure 3, please make the legends more clear. You should explain what the flow rates for various lines mean (total flow followed by the flow rates of dry and humidified flows at the inlet?). The green line in panel (b) has no dry/wet flow specification, why? Since the wall and inlet temperatures are the same in all panels, consider moving them into the figure caption.

9. Panel (b) of Figure 3 uses Kelvin as temperature units, but all other figures are in °C. For clarity, consider using the same units everywhere. The line showing the length of the tube (1 m) should be present in all panels, alternatively, you could consider truncating the simulation lines at 1 m axial

position.

We change the figures according to the suggestions of the reviewer.

10. Line 23: ...this can be also done on a short time scale (about 5 s) by controlling the ratio of the dry and the wet sheath air flow while the total flow is kept constant. In the beginning, you mentioned that there was no separate aerosol flow along the center of the tube, so what is the sheath flow for? Was the humidity of the sheath flow controlled separately? Where is this 5-second estimation coming from? Was it measured or simulated?

We agree with the reviewer that the statement of "sheath air" could be misleading. The reviewer is right, there is no separate aerosol flow along the tube center. There is only one particle-free gas flow along the tube. We delete the word "sheath".

The 5s estimation comes from a calculation, but was also measured by observing the ice crystals. For the calculation, we simply considered the total volume of the system downstream of the humidifier (not only the flow tube) and the flow rates.

11. Figure 4 and discussion thereof on page 5 casts many questions in conjunction with the data of figure 6: What are the solid lines: interpolation of numerical model results or something else? Was there wet flow in the model calculations and what were the wall boundary conditions? It appears to me that the measurements have been conducted under dry conditions, without ice coating the walls of the flow tube. Is that the case? Any idea why the measurements and model calculations deviate from each other at low wall temperature? Please address these issues thoroughly.

The solid lines in Fig. 4 and Fig. 6 are an interpolation of the experimental data - we add a note in the caption of the Fig. It is correct that there was no wet flow for the temperature characterisation data shown in Fig. 4. This means, the investigations have been done under dry conditions (by using pressurized air with a dew point slightly below -40°C). Using dry conditions holds for both, numerical simulations and measurements. The wall boundary condition in the simulations was zero flux. The reason for determining the temperature at dry conditions was that temperature measurements are not trivial under cold and wet conditions. For example, icing at the temperature sensor might occur. We know from wet simulations (with $S = 1$ at the wall boundary) that the temperature at the tube outlet is not significantly influenced by the presence of water in the system.

Furthermore, we also think that the differences between experimental data and simulation results are caused at least partly by the measurement technique. Especially at low flow velocities the temperature sensor, which was positioned in the optical measuring volume of LISA, several millimeters below the tube outlet, might not give true values. We spent much time using different types of sensors (various Pt100 and thermocouple sensors) to find out which one gives the best results for our application. In conclusion, even if the sensor is precisely calibrated (e.g. in an ethanol bath against a reference PT100 sensor), the difference between measurements and simulation results is probably due to technical measurement issues.

Measurements and simulations shown in Fig. 6 have been done for wet flow conditions. To minimize the effect of icing at the walls, the measurements were done only for a short time after the wet flow was switched on.

12. If the only purpose of Figure 5 is to demonstrate that IRIS ...can be used over a broad temperature range, please consider moving it into a supplementary material. It does not contribute to instrument characterization above what has been shown in Figure 4. Besides, it is unclear what are the solid lines on the color mapping.

We follow the suggestion of the Referee and move Fig. 5 into the supplement. We also add a figure to the supplement showing flow speed (measurements and simulations) data at the tube outlet. We change the text accordingly, delete the corresponding sentences (p. 5, l. 2-4) and add instead :

”Additionally, an extended data set of temperature measurements is shown in the supplement material.”

and in the previous section we change the last sentence to (p. 4, l. 31):

”Measured and calculated flow velocities were found to be very similar (see supplement material).”

13. Figure 6 and the discussion thereof on page 5: for the sake of comparison, please keep the same colors as in Figure 4 (red for $T_{\text{wall}} = -40^{\circ}\text{C}$ and so on).

There isn't one to one correspondence between the conditions in the two figures, hence the different colours. However, we followed the suggestion of the Reviewer and improved the Figs. for the revised version.

14. The deviation of measured RH_i values from FLUENT results is striking,

although FLUENT apparently makes a good job reproducing the flow temperature at the outlet (I am referring to the figure 4, the case of $T_{\text{wall}} = -30^{\circ}\text{C}$). There, FLUENT underestimates the temperature only by 1K, which translates into 10% difference of the water vapor pressure at this temperature but not into 20% as suggested by Figure 6! Also, why dont you show FLUENT results for other wall temperatures?

As stated in the reply to Point 6, the purpose of the simulations was to design the experiments. Therefore, the model was simplified in several ways. We reduced the flow simulations to a multicomponent (water + air), but single phase (gaseous phase) problems. Water phase transition was considered as a sink only. This means, the growing ice layer at the tube wall was not simulated. In the simulations, the wall boundary condition was defined by setting the walls to saturated conditions with respect to ice (100% at the wall temperature). Hence we are not able to simulate the temporal change of the saturation (and temperature) profile. However, one can imagine that a growing ice layer may act as an insulator increasing the temperature gradient. Additionally, the dry air flow was considered to be completely dry in the simulations (water mass fraction of zero), while the dew point of our pressurized air was in reality between about -50°C and -40°C . Simulation results are shown and compared to experimental data for the case of $T_{\text{wall}} = -30^{\circ}\text{C}$ because most the the experiments have been done at this temperature. For the data shown here, it is therefore the most relevant temperature value. Furthermore, measurements are getting more and more challenging at even lower temperatures. As stated above, temperature measurements at -40°C might be biased due to technical limitations. The same holds for dew point measurements. Therefore, we would expect that the differences between experiments and simulations results are a even bigger at -40°C .

15. Does the non-linearity of the measured RH_i data reflect the time evolution of the flow temperature field, as discussed on page 5, starting from the line 14? Have the measurements been taken by stepwise increasing the wet flow? Would you expect a different behavior if the wet flow was decreasing instead?

Yes, one reason for the non-linearity of the measured RH_i data is the time evolution of the temperatrue field. A second reason is the wall loss of water vapour at high RH. Water vapour is transported to the tube wall forming an ice layer. This sink also depresses the supersaturation. And yes, it is correct that the measurements were taken by increasing the wet flow. The temporal change of the temperature is not linear. We observed faster

changes at the beginning of the wall ice formation. At high RH_i ice is quickly formed at the wall. Therefore, at high RH_i there is not much difference if the measurements starts with a high wet flow. However, at low RH_i it is. We did measurements with decreasing wet flow showing a difference.

16. Page 6 line 6: I believe the correct name is Gray Level Co-occurrence Matrix (GLCM). I dont know what a co-matrix is. What is the definition of the image texture? How is it different from brightness distribution? A typical atmospheric scientist would know little to nothing about it.

The Reviewer is right, while the term co-matrix is often used for brevity in the literature, it is more correct to say "Co-occurrence Matrix"; we make a change in the text. See also response to Point 1.

17. Page 6 line 10 and on: since the concept of GLCM and its features is the central one in the manuscript, it would be nice to include a definition of GLCM energy which is used in the equation 1 to calculate the combined roughness but is not defined anywhere in the manuscript. This is even more so because the cited paper (Ulanowski et al., ACP 2014) does not provide any explanation of energy either, referring to the original paper by Haralik et al, 1973. However, Haralik et al. have not used the term energy among the statistical descriptors of image texture. It is therefore impossible for the reader to track down the definition of the term energy based on the provided information. Clarification of this issue is strongly advisable.

Incorrect: Haralick et al. do define "energy", just that this initial paper does not call it such. In any case, readers wishing to implement the measures can easily locate literally thousands of relevant references. However, for clarification we insert the text:

"(also known as uniformity, or angular second moment)"

18. A follow-up question to equation 1: The term combined roughness and the way it is discussed later suggest that this quantity describes both the irregularity (that is, the degree of deviation from a pristine habit) and the true physical surface roughness. Is that correct and if yes, what is their relative contributions?

This question cannot be answered at this stage, as the properties are not separable and anyway cannot be defined unambiguously. Further discussion is in the reference cited.

19. Page 6, line 21 and on: The method of size determination should be described in much more detail as it is given in the present form. For one, it is not clear at all if the size of the ice crystal has been always determined based on the analysis of the speckle area alone. The optical setup includes a microscope and the example microscope pictures definitely show that they were good enough to determine the size of the crystals within a few micron accuracy. This, however, is not mentioned explicitly. Even if the speckle area provides the necessary accuracy of size determination, one would certainly want to validate this method against the old-fashioned visual examination? This brings me to a question how exactly the size of the crystal has been retrieved from the speckle area? The only explanation in the manuscript is at the end of section 2.3, stating: In addition, the size of the ice particles, which is inversely proportional to the average area of speckle spots, is retrieved. However, the citing paper (Ulanowski et al., 2012) shows clearly that the relationship between the speckle area and size does not follow the simple inverse law (their equation 12 and figure 5). If the functional form of the relationship is not known, the only possibility that is left is to construct a calibration curve from the measurements where the crystal size is retrieved independently (using, for example, the optical microscope). Could you show such a curve? What are the uncertainties of size determination based on the speckle area analysis?

The method is described in detail and validated in the reference cited, which also includes a calibration curve. However, for clarification we insert the text:

”and is used throughout the present work to determine crystal size. The size measured in this way represents the diameter of equal area circle projected along the line parallel to the laser beam.”

See also response to Points 20 and 26.

20. On the other hand, the visual inspection is claimed to be used to [...] compensate for temporal changes of the thermodynamic conditions caused by the ice formation at the tube wall by adjusting the flow rate if the crystal growth slows down. These should be explained more clearly: were the microscope images used to control the growth rate of the ice crystal AND the speckle area analysis used to measure the crystal size in parallel? How do these two methods compare?

Since the characterization of the thermodynamic conditions was not precise enough to establish the point of equilibrium between the crystal and the vapour, we had to observe the crystal to find out whether it was growing or not, i.e. if it was in equilibrium. This established the point of reference. But otherwise the images were not used for adjusting the conditions. To clarify, we replace the last, potentially misleading sentence with the text:

”In this way the settings corresponding to the point of equilibrium between the crystal and the vapour can be found, to act as a reference point.”

The two methods cannot be directly compared because the crystal dimensions ”seen” by the two methods are orthogonal (one is parallel, the other perpendicular to the laser beam).

21. Page 6 line 25: [...] and the amount of speckle represents crystal roughness. This is one example where the roughness should be clearly defined. Are you talking about the roughness of the surface or combined roughness, which if I understand correctly, is the crystal irregularity plus surface roughness?

This was addressed previously, the roughness measure combines both. And the statement cited is a qualitative explanation, simply aiding the reader in the interpretation of unfamiliar 2-D scattering patterns.

22. Section 3 Results and discussion.

23. Figure 7 is a beautiful example of the 2D interference pattern produced by smooth and rough crystals. Could you show the corresponding microscope images of the crystals responsible for them?

While we agree with the Reviewer that the inclusion of images with Fig. 7 would be interesting, optical microscopy images (or cloud probe ones) do not reveal sufficient detail of surface roughness. Anyway, in this case parallel microscopy was not obtained, as the patterns were generated in a conventional cloud chamber. We now add an explanatory sentence in the caption:

”The patterns were produced using the SID3 instrument in the AIDA cloud chamber during growth at low (left) and high (right) supersaturation (Schnaiter et al., 2016).”

24. Page 7 line 26: Fast growth can moreover lead to the creation of de-

fects and ionization, ... what exactly do you mean by ionization? Charging, creation of the local or surface charge?

Please see the multiple references cited, which deal with this broad topic, as well as the Conclusions and the Reviewer's own Point 32.

25. Section 3.1. It is stated several times in the manuscript that the supersaturation could not be determined precisely due to the instability of the thermodynamic conditions in the flow tube. You are, nevertheless, able to estimate the supersaturation with an accuracy of around $\pm 5\%$ (as in lines 3 - 4 on page 8), which is not that bad for a highly dynamic system. Given the amount of effort that has been put into characterization of the flow tube and the fact that the supersaturation is indeed the key factor controlling the morphology of the ice crystals, I would suggest that you rewrite the characterization section clearly stating the range of supersaturation and the accuracy you could achieve but avoiding saying that the supersaturation could not be controlled. This creates unnecessary distrust in your results and shifts the focus of the discussion away from the physical mechanisms of surface roughening.

We did not say that supersaturation could not be controlled. In section 3.1 we state that "supersaturation ... could not be determined precisely". However, this may be misleading, so we now say "directly" instead, changing the sentence to:

"Since the supersaturation controls the growth rate but could not be determined directly with high accuracy in our experiments, ..."

26. Page 8 lines 8-9: The crystals can be compared directly as they grow from $20 \mu\text{m}$ to $29 \mu\text{m}$, after fitting trend curves using LOESS. What trend curves? What is LOESS? Was the size of the crystals determined from the speckle area analysis? What was the accuracy of such determination? Could you provide the confidence intervals for the LOESS fit? Would there be any growth in the confidence intervals for the slow growth case? What does raw in the legend of figure 8 mean: measurement points, raw data? Please be more specific and more careful in presenting the results!

LOESS is a well-established numerical technique, and is described and referenced earlier in the text. As for size, see Points 19 and 20. Concerning the "confidence intervals", these would not carry any information relevant to the behaviour of the observed crystal, as they are the outcome of sec-

ondary noise sources such as digitized image noise or mechanical vibrations, as pointed out in section 3.

27. Page 8 lines 17 - 28. I support the idea that nucleation of stacking disordered ice can be responsible for the formation of irregular crystals, but how does this relate to the surface roughness? I might remind the authors again that the title of the manuscript is Surface roughness during depositional growth...

Please see response to Point 1, it is stressed several times that we do not distinguish between fine and coarse. roughness.

28. Figure 9: Please use conventional way for naming the axis. The variables droughness and dsize are not defined anywhere in the text. Besides, what size is that: radius, diameter, characteristic size...?

The axes are defined as rates in the caption, and the variables "roughness" and "size" in the text, see also response to Point 19 above. However, for clarity we alter the axis labels to "d(roughness)/d(time)" and "d(size)/d(time)".

29. Page 10 lines 8 - 9. Careful examination of the retrieved crystal size shown in Fig 10 indicates markedly slower growth in later cycles, despite similar supersaturation levels. To my opinion, this is stretching the imagination too far. There are only two growth cycles delivering comparable data, and the difference in the growth slope can be caused by anything else. How similar are the supersaturation values? Was the size change confirmed by optical microscope? Why does the same behavior not show up in Figure 11?

The supersaturations were the same. We bring this observation to the readers attention as it is potentially important, and we do not claim it as a "fact", hedging our bets with words like "appears to" etc. However, we cite similar behaviour observed in other systems. Moreover, concerning Fig. 11, we beg to disagree, as similar behaviour can be seen in crystal growth rate. So we are prepared to stand by our statements, and further work will confirm or contradict them. As for the microscopy, see response to Point 20.

30. One more comment on this point. To my understanding, the growth rate based on the optical size, as derived from the speckle area analysis, is directly related to the rate of growth of a volume equivalent diameter (or any other characteristic size describing the envelope dimension of the crystal). The growth rate based on such equivalent diameter is directly

proportional to the mass growth rate. As combined roughness increases (as you have shown nicely), the ratio of surface to mass increases too, meaning that creating more surface in case of a growing complex crystal does not contribute to mass growth in the same way as in case of a growing pristine hexagonal column or plate. What implication this effect would have for the atmospheric phenomena is a question which, I am afraid, cannot be answered without thorough modeling of crystal growth with the cloud microphysical feedbacks.

No, it is not "volume equivalent diameter" - see Point 19. However, we are happy to support the rest of the Reviewer's comment.

31. Page 11 line 2-3: It is very likely, as shown in our experiments, that at higher supersaturation rougher crystals will develop at the expense of smoother ones. I strongly doubt it. What would be the mechanism of such competition? Would you expect the pressure difference above smooth and rough surfaces? If not, why would rough crystals grow preferentially if both rough and smooth crystals are exposed to a supersaturated water vapor? Please clarify this statement or remove from the discussion.

We merely reiterate that our experiments show higher roughness at high supersaturation, and that this is also likely to occur in the atmosphere. However, to avoid misunderstanding, we change the words "develop at the expense of" to "tend to develop instead of".

32. Page 11 line 22 and on: Finally, we note that rough ice surfaces are associated with stronger electrical charging (Caranti and Illingworth, 1983; Dash et al., 2001; Dash and Wettlaufer, 2003), hence the presence of roughness may influence storm electrification. This is indeed very interesting link that is worth discussing in more detail. Could you say a few words explaining what mechanism underlay this phenomenon? I think this is the most far leading mechanism among other atmospheric applications.

This is indeed an intriguing possibility, that is why we speculatively mention it. However, we consider wider discussion to be beyond the scope of the present work, and we instead refer the readers to several references cited in sections 3.1 and 3.3.

Responses to Referee #3

”Surface roughness during depositional growth and sublimation of ice crystals” *by Cédric Chou et al.*

This unique laboratory study combines a laminar flow tube with a laboratory version SID-3 instrument, where flows from a dry and a wet laminar flow tube are mixed to control the supersaturation characterizing ice crystal growth at the flow tube outlet where SID-3 measurements are made (including microscope imagery). The methodology is adequately explained while the results are well explained, and the paper is well organized. The results advance our knowledge of the dependence of ice particle optical properties on ice growth/sublimation processes. I did not find much to criticize in this study.

We thank the Referee for the positive comments and suggestions. Below we list our response to the two main comments.

Specific Comments:

1. Page 5, line 2 regarding Fig. 4: The measurements agree well with the Fluent calculations except at -40°C at low flow rates. Please suggest reasons for these differences.

We think that the reason for the deviation between measurements and simulations at low temperatures and (especially) low flow rates are caused by the measurement technique. Accurate temperature measurement in a gas flow under a small flow tube at low flow temperature and flow speed is not trivial. The temperature sensor, which was positioned in the optical measuring volume of LISA several millimeters below the tube outlet, might not give accurate values if the flow velocity is too small, especially at low temperatures. We spent a lot of time using different types of sensors (various Pt100 and thermocouple sensors) to find out which one gives the best results for our application. In conclusion, even if the sensor is precisely calibrated in an ethanol bath against a reference Pt100 sensor, the difference between measurements and simulation results is probably due to technical measurement issues.

2. Page 9, lines 15-16: these observations indicate that the more growth-sublimation cycles are performed, the rougher the crystal can become. Figure 11 does not seem to support this. Rather, the 3rd maximum in surface roughness in Fig. 11 (corresponding to the 3rd growth cycle) is slightly lower on average than the 2nd maximum in Fig. 11 (although both maximums are comparable). Therefore, it appears possible that a limiting roughness threshold exists that would not be exceeded in subsequent growth-sublimation cycles. This possibility should be acknowledged. Such a possibility seems consistent with our theoretical understanding of ice crystal surface kinetics and growth processes. Moreover, future work should explore this possibility by analyzing 3 or more continuous growth-sublimation cycles in multiple experiments at various wall temperatures. If a laboratory roughness threshold were established (possibly being supersaturation- and temperature-dependent), then the next logical step would be to look for evidence of this in natural cirrus clouds. Quantifying and bounding the degree of ice crystal surface roughness is needed to reduce uncertainty in the cirrus cloud radiative effect (CRE) in climate models.

We stopped the experiments after a few growth-sublimation cycles because the gross shape of the ice crystals often slightly changes with each cycle. Here, we didn't wish to mix the effects of surface roughness and larger irregularities and therefore stopped when the ice crystal started to develop significantly different morphology. So we generally agree with the Reviewer's point that there appears to be an upper limit of the (combined) roughness value, but higher values could be reached in principle during longer experiments. We consider this suggestion and will try to address this point in future investigations.

Technical Comments:

1. Page 3, line 23: space between the and central.
2. Page 16, lines 19-21: Reference cited incorrectly. Title should be Cloud chamber experiments on the origin of ice crystal complexity in cirrus clouds, and the year of publication should be 2016. I have not checked other references; the authors should check these too.
3. Figure 3: In lower panels, the y-axis labels should be changed from ration to ratio. Regarding saturation profile panel b, should %5 l/min be 5 l/min?
4. Figure 4: Flow units are in dl/min; should this be l/min? If not, define dl.

We improve the Figs. as suggested and have rechecked the references.

Surface roughness during depositional growth and sublimation of ice crystals, by Cedric Chou et al.

List of major changes

Key: insertions are in blue, deletions are ~~crossed-out in red~~. The page and line numbers refer to the original discussion paper.

2.1 Experimental setup

P.2 line 31: In the experiments, the ice crystals, **generally single**, are fixed within the measuring volume

P.3 line 28: via an Infinitube right-angle adaptor with fibre-optics **in-line** illumination

2.1.1 Laminar flow tube

P.3 line 10: mass flow controllers (~~MFC~~, Brooks 5850s, Brooks Instruments, Hatfield, PA, USA)

2.1.2 Optical system

P.3 line 23: 2-D scattering patterns are collected by LISA via an intensified CCD camera at scattering angles from 6 to 25° in an annular shape, which ensures that the **bright feature associated with the familiar halo occurring for ice prisms at the scattering angle of 22°** ~~halo-scattering from ice prisms~~ is included. The ~~lower angles in the central~~ **smaller angles in the central** area are not captured due to the presence of a beam stop.

~~2.1.3 Operating principle~~

2.2 Numerical simulations and thermodynamic characterisation

P.4 line 2: ~~To illustrate the operating principle of IRIS, simulation results are shown in Fig. 3. These simulations, which were originally used to design the experiments,~~ The thermodynamic conditions at the tube outlet were extensively studied by means of computational fluid dynamics (CFD) 5 simulations of the laminar flow tube, and by measurements of flow velocity, temperature and dew point at the tube outlet. Both the numerical simulations and the measurements have been done to characterise the experimental setup, as well as to demonstrate the fast control of temperature and supersaturation in the measuring volume.

The numerical simulations were done with the commercially available CFD code Fluent (Ansys Inc., USA). The Fluent model is a general purpose FVM (finite volume method) CFD model allowing the simulation of a wide range of small scale 10 fluid flow problems. Here, the flow through the flow tube was simulated including the coupled processes of mass and heat transfer. With respect to the geometry and the laminar flow regime, the simulations were done on a 2-dimensional axisymmetric Cartesian grid by means of a pressure based steady state solver. With respect to the geometry and the laminar flow regime, the simulations were done on a 2-dimensional axisymmetric Cartesian grid by means of a pressure based steady state solver. Additional information about the numerical model, which has already been successfully applied to the characterisation of the laminar flow tube LACIS, can be found for example in Stratmann et al. (2004); Voigtländer et al. (2007) and Hartmann et al. (2011).

To illustrate the operating principle of the laminar flow diffusion channel, calculated thermodynamic profiles along the tube axis are shown in Fig. 3.

~~For a sufficiently high gas flow representing~~ If the residence time of the gas flow, ~~the thermodynamic~~ (controlled by the mass flow rate) is large enough, the gas flow cools down until thermodynamic equilibrium with the tube wall is reached. Conversely, for a sufficiently fast flow equilibrium ~~between the wall and the gas flow~~ will not be reached.

P.4 line 23: by controlling the ratio of the dry and the wet ~~sheath~~ air flow while the total flow is kept constant.

~~2.2.1 Thermodynamic characterisation~~

P.4 line 30: Measured and calculated flow velocities were found to be very similar (~~not shown here see supplement material~~).

P.5 line 2: ~~Fig. 5 shows an extended dataset of measured temperatures between 0°C and -40°C supplemented by interpolated values illustrating that IRIS can be used over a broad temperature range~~ Additionally, an extended data set of temperature measurements is shown in the supplement material.

P.5 line 26: This is done by ~~continuous~~ observation of the ice crystal with the optical microscope. Since the ice crystal growth process is highly sensitive to the prevailing thermodynamic conditions, i.e. the saturation ratio determines the ice crystal growth rate, the ~~MFCs massflowcontrollers~~ can be adjusted according to the microscope images. In ~~other words, the camera images are used to compensate for temporal changes of the thermodynamic conditions caused by the ice formation at the tube wall~~ this way the settings corresponding to the point of equilibrium between the crystal and the vapour can be found, to act as a reference point.

2.4 Scattering pattern analysis

P. 6 line 7: In brief, image texture can be retrieved by using the ~~grey-level-co-matrix~~ Grey-Level Co-occurrence Matrix (GLCM)

P. 6 line 10: among the four features of the GLCM (contrast, correlation, ~~energy and homogeneity~~ homogeneity and energy, also known as uniformity or angular second moment),

P. 6 line 16: where ~~E-E~~ is the energy derived from the GLCM and ~~K K~~ the kurtosis. ~~This~~ The combined measure is dependent on the number of independent “scattering centres”

P. 6 line 20: In addition, the size of the ice particles, which is inversely proportional to the average area of speckle spots, is retrieved and is used throughout the present work to determine crystal size. The size measured in this way represents the diameter of equal area circle projected along the line parallel to the laser beam (Ulanowski et al., 2012).

P. 6 line 22: The presence of isolated bright spots or bands is an indication of flat crystal facets, while spots covering a large proportion of the pattern signify the presence of roughness or high

3 Results and Discussion

P. 6 line 28: In the following, ~~first~~ experiments are presented and discussed ~~first~~, addressing two aspects; ~~the influences~~ the influence of supersaturation, and of regrowth cycles on the ice crystal surface roughness measures. However, we note that in general other factors may also influence crystal morphology

P. 7 line 8: Fig. 6 shows examples of ~~a smooth and rough~~ 2-D scattering patterns ~~of from smooth and rough ice~~ columns to illustrate what patterns could be classified as ~~originating from~~ smooth or rough ice crystals in the following discussion.

3.1 Slow and fast growth

P. 7 line 26: Fast growth can moreover lead to the creation of defects and ionization, which further promote irregular growth (Beckmann, 1982; Dash et al., 2001; Dash and Wettlaufer, 2003; Pantarakis and Flood, 2005; Ferreira et al., 2008; Flood, 2010).

P. 7 line 33: Since the supersaturation controls the growth rate but could not be determined ~~precisely~~ directly with high accuracy in our experiments

P. 8 line 4: The slow growth experiments were done ~~closeer~~ closer to saturated conditions (typically about 5% supersaturation wrt. ice).

3.2 Roughness due to humidity cycles

P. 8 line 30: Another process that could influence the roughness of ice crystals is the exposure to several depositional growth and sublimation cycles ~~(Nelson, 1998; Korolev et al., 1999)~~, which can occur in the atmosphere (Nelson, 1998; Korolev et al., 1999; Ulanowski et al., 2014).

P. 9 line 28: the cyclic growth described here tended to result in a ~~slight~~ reduction in roughness during each sublimation phase.

P. 9 line 29: The apparent disparity between our observations and SEM experiments can be accounted for by the fact that growth in the absence of air that takes place in a SEM chamber, instead of being ~~diffusion-limited~~ limited by vapour diffusion as is the case for ice at tropospheric pressures, becomes limited by the attachment kinetics ~~(Libbrecht, 2017)~~. This distinction is known to lead to different growth rates as well as habits (Beckmann, 1982; Kuroda and Gonda, 1984; Libbrecht, 2017). Consequently, during SEM observations water molecule removal can take place anywhere on facet surfaces, leading to pronounced roughness. Moreover, the bunching of elementary molecular steps, possibly due to the Schwoebel effect (Misbah et al., 2010), can result in the creation of larger, microscopic (as opposed to elementary) steps that can be seen in SEM micrographs (Cross, 1969).

P. 10 line 3: A further difference between the diffusion limited and kinetics-limited growth is that the former can lead to increased numbers of faults (Beckmann, 1982) and dendritic, skeletal, or needle-shaped crystals, while the latter tends to produce more perfect, smooth, isometric prisms (Gonda, 1976, 1977)

3.3 Atmospheric Implications

P. 11 line 2: It is very likely, as shown in our experiments, that at higher supersaturation rougher crystals ~~will develop at the expense~~ tend to develop instead of smoother ones

Author contributions: C.C, J.V., P.H., H.B. designed and carried out the experiments including sample preparation and data analysis with assistance from T.C. J.V. performed the computational fluid dynamics simulations. Z.U. conceived and supervised the project and provided crystal property measurement techniques and interpretation of ice growth processes. F.S., Z.U, J.V. developed the main conceptual ideas and the technical details of the experiments and the

experimental setup IRIS. C.C., J.V., Z.U. wrote the manuscript with support from P.H., H.B., F.S., T.C., D.N., S.H. and G.R. All authors discussed the results.

Acknowledgements: This work was supported by the UK Natural Environment Research Council grant NE/I020067/1 (ACID-PRUF) and the EU Eurochamp-2 scheme grant E2-2011-12-06-0065. The concept of LISA was proposed by Alexei Kiselev, and the instrument itself was designed and built by Edwin Hirst at the University of Hertfordshire.

References

Beckmann, W.: Interface kinetics of the growth and evaporation of ice single crystals from the vapour phase: III. Measurements under partial pressures of nitrogen, *J. Cryst. Growth*, 58, 443–451, doi:10.1016/0022-0248(82)90291-3, 1982.

Kuroda, T., and Gonda, T.: Rate determining processes of growth of ice crystals from the vapour phase, Part II: investigation of surface kinetic processes, *J. Meteor. Soc. Jap.*, 62, 563–572, doi:10.2151/jmsj1965.62.3_563, 1984.

Misbah, C., Pierre-Louis, O., and Saito, Y.: Crystal surfaces in and out of equilibrium: A modern view, *Rev. Mod. Phys.*, 82, 981-1040, doi:10.1103/RevModPhys.82.981, 2010.

Figures

Figure 4. Comparison between measured and calculated temperature in dependence of the total flow rate using three different wall temperatures. The solid lines represent interpolation of the experimental data.

~~Figure 5. Measured temperatures in the observation volume of LISA. Measuring points are represented by the black dots and the coloured contours are interpolated values.~~

Figure 6. 2-D scattering ~~pattern patterns~~ of a smooth column (left panel) and a rough column (right panel). The patterns were produced using the SID3 instrument in the AIDA cloud chamber during growth at low (left) and high (right) supersaturation (Schnaiter et al., 2016).

Supplements S3, S4 and S5 (PLEASE NOTE: Figures S3 and S4 are new, Figure S5 was previously Figure 5 in the main text)

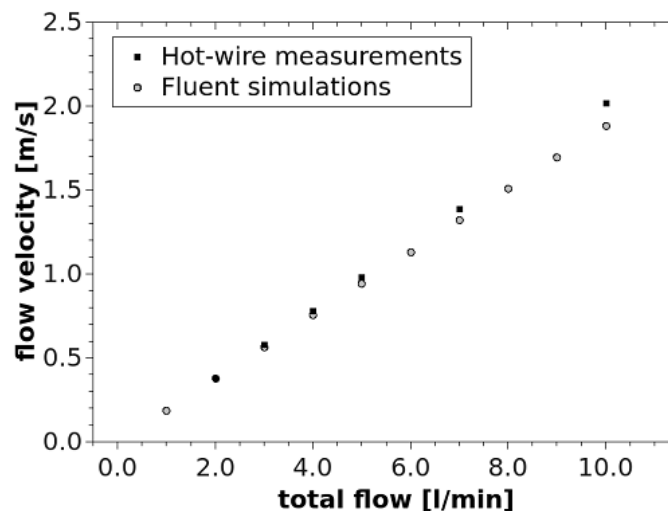


Fig. S3. Measured and simulated velocity at the center outlet of the laminar flow diffusion chamber with respect to the total flow. The measurements were done by means of an hot-wire anemometer (Dantec Dynamics, Denmark). The miniature hot-wire sensor (Dantec 55P11 sensor) was fixed at the tube outlet in the measuring volume of the laser beam. Single point measurements were done in dependence of the total flow. The data were compared to Fluent simulation results. Both measurements and simulations were done at 20° and dry conditions.

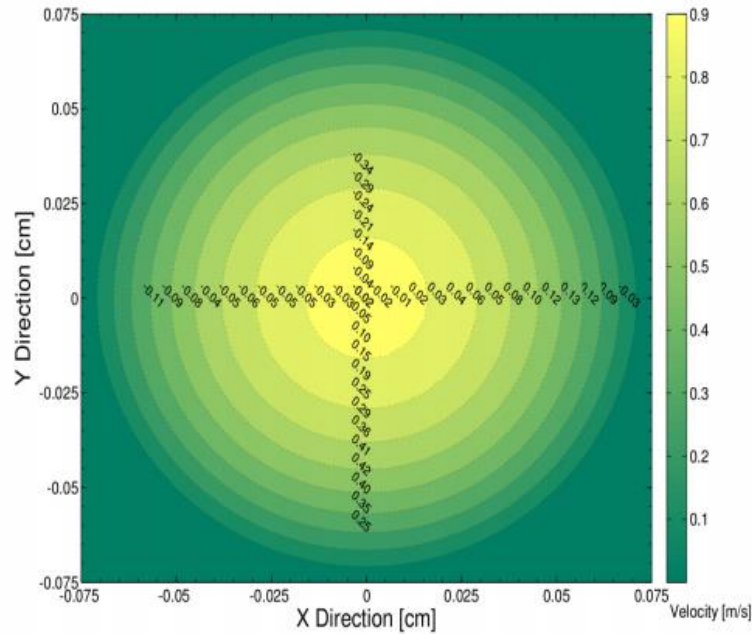


Fig. S4. Illustration of calculated velocity data (contour plot of Fluent simulation results) and the difference between measurements and calculations (values). The position of the numbers corresponds to the measurement position of the hot-wire sensor in the cross sectional profile at the tube outlet.

~~Figure 5. Measured temperatures in the observation volume of LISA. Measuring points are represented by the black dots and the coloured contours are interpolated values.~~ Fig. S5. Contour plot of the temperature characterization results. The figure was obtained by a linear interpolation of the temperature measurements (black dots). The black lines are temperature isolines. The figure illustrates that IRIS can be used over a broad temperature range.

Surface roughness during depositional growth and sublimation of ice crystals

Cedric Chou^{1,2,*}, Jens Voigtländer^{3,*}, Zbigniew Ulanowski¹, Paul Herenz³, Henner Bieligk³, Tina Clauss^{3,4}, Dennis Niedermeier³, Susan Hartmann³, Georg Ritter¹, and Frank Stratmann³

¹School of Physics Astronomy and Mathematics, University of Hertfordshire, Hatfield, AL10 9AB, UK

²Department of Medicine, University of British Columbia, Vancouver, BC, Canada

³Leibniz Institute for Tropospheric Research, Permoserstr. 15, 04318 Leipzig, Germany

⁴DBFZ — Deutsches Biomasseforschungszentrum, Torgauer Str. 116, 04347 Leipzig, Germany

*These authors contributed equally to this work

Correspondence: Joseph Z. Ulanowski (z.ulanowski@herts.ac.uk)

Abstract. Ice surface properties can modify the scattering properties of atmospheric ice crystals and therefore affect the radiative properties of mixed-phase and cirrus clouds. The Ice Roughness Investigation System (IRIS) is a new laboratory setup designed to investigate the conditions at which roughness develops on single ice crystals, based on their size, morphology and growth conditions (relative humidity and temperature). Ice roughness is quantified through the analysis of speckle in 2-D light scattering patterns. Characterisation of the setup shows that a supersaturation of 20% with respect to ice and a temperature at the sample position as low as -40°C could be achieved within IRIS. Investigations of the influence of humidity show that higher supersaturations with respect to ice lead to enhanced roughness and irregularities of ice crystal surfaces. Moreover, relative humidity oscillations lead to gradual “ratcheting up” of roughness and irregularities, as the crystals undergo repeated growth-sublimation cycles. This memory effect also appears to result in reduced growth rates in later cycles. Thus, growth history, as well as supersaturation and temperature, influences ice crystal growth and properties, and future atmospheric models may benefit from its inclusion in the cloud evolution process, and allow more accurate representation of not just roughness but crystal size too, and possibly also electrification properties.

1 Introduction

Cloud properties and their effects remain the largest uncertainty in global climate models (Boucher et al., 2013). In particular, climate feedbacks of cirrus clouds, which cover 30% of the globe (Wylie et al., 2005) and 60-70% in the tropics (Sassen et al., 2009), are still not well understood. The main reasons of these uncertainties lie in the fact that ice crystals which compose cirrus clouds have widely varying morphology, size and concentration (McFarquhar and Heymsfield, 1997; Heymsfield et al., 2017) and therefore have different scattering properties, influencing in turn the radiative properties of the clouds (Hartmann et al., 1992; McFarquhar et al., 2000; Baran, 2012; Yang et al., 2015). Several cloud imaging probes like the Cloud Imaging Probe (CIP), Cloud Particle Imager (CPI) or various optical array probes (e.g. 2DC, 2DS) among others, have been developed over the last decades in order to characterise those parameters. However, these probes have difficulties characterising the size and shape

of smaller ice crystals, due to optical resolution limitations. Moreover, these probes do have a further limitation due to varying degree of shattering of ice particles on their inlets, only partly reduced by various mitigation measures (Ulanowski et al., 2004; Field et al., 2006; Connolly et al., 2007; Jensen et al., 2009; Korolev et al., 2011; Baumgardner et al., 2017). For these reasons, a new family of probes called collectively Small Ice Detector has been developed, which has open-path detection geometry
5 designed to reduce shattering, and relies on retrieving particle size and shape from scattering patterns instead of images (Kaye et al., 2008; Cotton et al., 2010; Ulanowski et al., 2014).

Further to the challenge of retrieving the size distribution and concentration of small ice crystals present in clouds, it has been shown on the basis of light-scattering models that irregularities of ice crystal surfaces, such as roughness and concavity can affect the light scattering properties (Yang et al., 2008b, a; Liu et al., 2013). Experiments performed on ice analogues have
10 shown that the asymmetry parameter of large ice analogue crystals possessing surface irregularities can be over 20% lower at visible wavelengths in comparison to smooth counterparts (Ulanowski et al., 2003, 2006). This in turn can result in large reductions in shortwave radiative forcing (Yi et al., 2013). Suggestions that atmospheric ice may depart from the idealized hexagonal crystal model have been made for several decades (Foot, 1988; Korolev et al., 1999; Auriol et al., 2001; Garrett et al., 2001) and there is now accumulating evidence that natural ice clouds can contain a significant proportion of, or can even
15 be dominated by, ice particles that substantially depart from the idealized smooth, hexagonal prism shape – for reviews and recent results see Ulanowski et al. (2014), Yang et al. (2015) and Hioki et al. (2016). Recent in-cloud measurements using the Small Ice Detector 3 (SID-3) during CONSTRAIN (Ulanowski et al., 2014) and MACPEX (Schmitt et al., 2016) have shown that most of the ice crystal encountered could be classified as rough. However, the conditions that lead to the development of crystal irregularities are still not well understood, because previous ice growth experiments tended to focus on growth rates and
20 crystal habits, rather than the fine detail that can contribute to light scattering properties.

To study the influence of growth conditions on ice crystal roughness, laboratory experiments simulating atmospherically relevant depositional growth and sublimation of ice crystals are required. In the present study, the newly developed experimental setup IRIS (Ice Roughness Investigation System) is introduced, which facilitates the exposure of a fixed ice crystal to different controlled relative humidities and temperature regimes. The system is used to carry out ice crystal growth experiments at
25 different supersaturation ratios, and to investigate the impact of repeated growth and sublimation cycles on surface roughness. The findings are discussed in the context of fundamental features of ice crystal growth and their atmospheric implications.

2 Methodology

2.1 Experimental setup

The experimental setup is a combination of a laminar flow tube and a laboratory version of the SID-3 instruments, which
30 has been additionally equipped with an optical microscope. The laminar flow tube is used to precisely control the thermodynamic conditions in the optical measuring volume at the tube outlet. In the experiments, the ice crystals, generally single, are fixed within the measuring volume and exposed to thermodynamic conditions simulating single or multiple growth cycles at

various temperature and saturation ratio. A brief description of the setup, the operating principle and the thermodynamical characterisation is given in the following subsections.

2.1.1 Laminar flow tube

The laminar flow tube follows the principle of the Leipzig Aerosol Cloud Interaction Simulator (LACIS Stratmann et al. (2004);
5 Hartmann et al. (2011)). It has been further developed to provide required conditions with respect to humidity and temperature at the outlet where the ice crystal is situated. The main part is a thermodynamically controlled laminar flow tube with a diameter of 15 mm and a length of 1.0 m. Both, the wall and the inlet temperature of the insulated flow tube can be precisely controlled by means of thermostats, which are operated in counter flow direction. The main differences between LACIS and IRIS are the extended mass flow range and the missing separated aerosol beam. The mass flow is adjusted by means of two
10 mass flow controllers (~~MFC~~, Brooks 5850s, Brooks Instruments, Hatfield, PA, USA), controlling a dry (dew point between -60°C and -40°C) and a humidified gas flow in the range between 1 and 10 l/min standard temperature and pressure (STP), respectively. The humidification of the wet flow is done by water vapour transport through a micro-porous Nafion (sulfonated tetrafluoroethylene based fluoropolymer-copolymer) membrane. By operating the water cycle of the humidifier in counter flow direction, the air flow reaches a relative humidity (RH) of $100\pm 0.03\%$ at equilibrium. Both flows are combined in a small
15 mixing bottle before entering the tube to ensure a well-mixed gas flow. The dew point temperature at the tube inlet then is defined by the mixing ratio and the dew points of both flows. A simplified schematic of the experimental setup is given in Fig. 1.

2.1.2 Optical system

The Leipzig Ice Scattering Apparatus (LISA) is a laboratory version of the Small Ice Detector 3 (SID-3, also known in its
20 other laboratory version as the Particle Phase Discriminator - PPD), which allows the differentiation of ice crystals from water droplets, as well as ice crystal size and shape characterisation (Kaye et al., 2008). In addition, it also allows the characterisation of ice crystal irregularities on the basis of the two-dimensional (2-D) speckle pattern distribution (Ulanowski et al., 2014). 2-D scattering patterns are collected by LISA via an intensified CCD camera at scattering angles from 6 to 25° in an annular shape, which ensures that the bright feature associated with the familiar halo occurring for ice prisms at the scattering angle
25 of 22° -halo scattering from ice prisms is included. The ~~lower angles in the central~~ smaller angles in the central area are not captured due to the presence of a beam stop. The camera images are digitized as 12-bit TIFF files allowing a wider dynamic range with a fixed intensifier gain value, as opposed to the 8-bit JPEG files used during CONSTRAIN (Ulanowski et al., 2014). In addition, a CMOS camera (Prosilica GC1280, Allied Vision Technologies, USA) attached to a 20-times magnification long working-distance microscope objective (20x Mitutoyo Plan Apo) via an Infinitube right-angle adaptor with fibre-optics in-line
30 illumination (Infinity Photo-Optical Company, USA) was added to LISA in order to visualise the evolution of the ice crystal. Ice crystals were monitored by the camera at 27 frames per second, ensuring no loss of information during fast humidity cycles. Fig. 2 shows a simplified schematic of LISA.

2.1.3 Operating principle

2.2 Numerical simulations and thermodynamic characterisation

To illustrate the operating principle of IRIS, simulation results are shown in Fig. 3. These simulations, which were originally used to design the experiments,

5 The thermodynamic conditions at the tube outlet were extensively studied by means of computational fluid dynamics (CFD) simulations of the laminar flow tube, and by measurements of flow velocity, temperature and dew point at the tube outlet. Both the numerical simulations and the measurements have been done to characterise the experimental setup, as well as to demonstrate the fast control of temperature and supersaturation in the measuring volume.

The numerical simulations were done with the commercially available CFD code Fluent (Ansys Inc., USA). The Fluent model is a general purpose FVM (finite volume method) CFD model allowing the simulation of a wide range of small scale fluid flow problems. Here, the flow through the flow tube was simulated including the coupled processes of mass and heat transfer. With respect to the geometry and the laminar flow regime, the simulations were done on a 2-dimensional axisymmetric Cartesian grid by means of a pressure based steady state solver. Additional information about the numerical model, which has already been successfully applied to the characterisation of the laminar flow tube LACIS, can be found for example in Stratmann et al. (2004); Voigtländer et al. (2007) and Hartmann et al. (2011).

To illustrate the operating principle of the laminar flow diffusion channel, calculated thermodynamic profiles along the tube axis are shown in Fig. 3. Generally, the thermodynamic conditions in the measuring volume at the flow tube outlet depend on mass and heat transfer to the tube wall. Since the tube wall temperature is adjusted to lower values than the inlet temperature the gas flow temperature along the tube axis decreases due to heat conduction (Fig. 3, top right). Depending on both the temperature gradient and the inlet dew point, supersaturation with respect to water and/or ice can be achieved (Fig. 3, bottom). For a sufficiently high gas flow representing If the residence time of the gas flow, the thermodynamic (controlled by the mass flow rate) is large enough, the gas flow cools down until thermodynamic equilibrium with the tube wall is reached. Conversely, for a sufficiently fast flow equilibrium between the wall and the gas flow will not be reached. Consequently, the thermodynamic conditions at the tube outlet are determined by the total mass flow, the wall and inlet temperatures, as well as the inlet saturation ratio. Fig. 4 shows that for a total flow rate between 4 and 10 l/min, an inlet temperature of 20°C and a wall temperature of -30°C, the temperature at the tube centre outlet increases almost linearly by about 10°C with increasing flow. As a consequence the temperature in the measuring volume can be varied by at least 10°C on a very short time scale (about 2 s) by varying the total flow rate. In contrast, the temperature values for a flow rate smaller than about 3 l/min indicate that the residence time becomes sufficiently long to approach the thermodynamic equilibrium state. In this case, the thermodynamic conditions can no longer be controlled by varying the flow rate. Since control of the conditions by adjusting the thermostats (wall and inlet temperatures) is much slower, a flow rate of about 3-4 l/min represents the lower practical limit for the experiments. Because temperature is usually kept constant in typical experiments, the saturation ratio is controlled by varying the inlet dew point. As mentioned before, this can be also done on a short time scale (about 5 s) by controlling the ratio of the dry and the wet sheath air flow while the total flow is kept constant.

2.2.1 Thermodynamic characterisation

The thermodynamic conditions at the tube outlet have been extensively characterised using measurements of the flow velocity, temperature and dew point. The flow characterisation was done applying hot wire anemometry (Dantec Dynamics A/S, Skovlunde, Denmark). By means of a miniature, single-axis probe, the velocity magnitude was determined at several points
5 along a cross sectional profile of the tube outlet showing a parabolic laminar velocity profile without any back flows. In the measuring volume, the flow velocity increases linearly from approx. 0.5 to 2.0 m/s for total flow rates between 3 and 10 l/min. For typical experimental conditions with flow rates around 5 l/min the resulting flow velocity is about 1 m/s. Measured and calculated flow velocities were found to be very similar (~~not shown here~~[see supplement material](#)).

Temperature measurements were done at the outlet of the laminar flow chamber using calibrated (to an accuracy of ± 0.01 K.)
10 external resistance thermometers Pt100, as well as K-type thermocouple sensors. Fig. 4 shows measured temperatures as a function of the total volume flow at selected wall temperatures (-20°C , -30°C and -40°C) in comparison to Fluent simulation data for an inlet temperature of 20°C . It can also be seen that both data sets are in a good agreement. ~~Fig. ?? shows an extended dataset of measured temperatures between 0°C and -40°C supplemented by interpolated values illustrating that IRIS can be used over a broad temperature range~~[Additionally, an extended data set of temperature measurements is shown in the supplement](#)
15 [material](#).

The dew point temperature (respectively frost point temperature and relative humidity) was characterised using a dew point mirror (model Dew Point Mirror 973, MBW Calibration, Wettingen, Switzerland). An example of measured relative humidity with respect to ice (RH_i) is shown in Fig. 5. Therein, the RH_i is depicted in dependence of the wet flow. In this example, which represents typical experimental conditions, the wall temperature was at -30°C , the inlet temperature at 20°C , and the
20 inlet dew point temperature at 19.5°C . The total flow was kept at a constant value of 5 l/min. According to Fig. 4 ~~and Fig. ??~~, the resulting temperature was about -27.5°C . The saturation ratio rises steeply with increasing fraction of the humidified flow. Fig. 5 demonstrates that the saturation ratio in the measuring volume can be varied between sub- and supersaturated conditions (with respect to both water and ice). Here, the saturation ratio with respect to ice ranges from 0.75 (0.1 l/min wet flow) up to 1.2 (2 l/min wet flow).

25 In the experiments it was also found that for low wall temperatures and supersaturated conditions (with respect to ice) the conditions in the sampling volume changed slowly with time. Thereby, the lower the wall temperature and the higher the supersaturation, the faster the conditions in the tube change. Consequently, experiments at very high saturation ratios (>1.20 wrt. ice) were avoided. Due to ice formation at the tube wall, the observed temperature and the dew point increased at the tube outlet. This is most likely caused by the growing ice shell at the tube wall, which acts as a thermal insulator suppressing
30 the temperature gradient and hence the diffusional processes in the flow tube. For example, considering a wall temperature of -40°C , a total flow of 7 l/min and a wet flow of 0.9 l/min, resulting in a saturation ratio of about 1.2 with respect to ice in the beginning, the temperature increases from about -31.7°C to -31.0°C and the frost point from about -29.5°C to -29.0°C within 20 min. Fluctuations of both the temperature and the dew/frost point have an impact on the saturation ratio and therefore on the growth rate of the observed ice crystal, the ice layer at the tube wall can also act as an extra source for water vapour, if

the conditions are changed from super- to subsaturated conditions. It has to be concluded that for supersaturated experiments, a detailed quantitative characterisation of the saturation ratio on the basis of dew point measurements is not possible and that additional methods are needed to evaluate the saturation ratio during the experiments. This is done by ~~continuous~~ observation of the ice crystal with the optical microscope. Since the ice crystal growth process is highly sensitive to the prevailing thermodynamic conditions, i.e. the saturation ratio determines the ice crystal growth rate, the ~~MFCs~~ mass flow controllers can be adjusted according to the microscope images. In ~~other words, the camera images are used to compensate for temporal changes of the thermodynamic conditions caused by the ice formation at the tube wall~~ this way the settings corresponding to the point of equilibrium between the crystal and the vapour can be found, to act as a reference point.

2.3 Sample preparation

10 Laboratory investigation of ice crystal surface properties requires the formation of the initial ice crystal from a foreign particle termed an ice nucleating particle (INP). For experiments done at IRIS, a single INP is attached to the tip of a thin glass fibre. These very thin tips of about $2\ \mu\text{m}$ in diameter were pulled from 1 mm diameter borosilicate rods using a micropipette glass puller. The glass was cleaned and hydrophobically coated following the procedure described by Dymarska et al. (2006). The glass fibre was then attached to a micromanipulator (Singer Mk.1, Singer Instruments, UK) which was used to pick the INP
15 (usually of several micrometres in size) that had been deposited on a microscope glass slide under a microscope (Zeiss Primo Vert, Germany).

2.4 Scattering pattern analysis

The 2-D scattering patterns are characterised by quantifying their brightness distributions and texture (Ulanowski et al., 2014). In brief, image texture can be retrieved by using the ~~grey-level co-matrix~~ Grey-Level Co-occurrence Matrix (GLCM) which
20 consists of pairing each grey-level pixel with the nearest neighbour pixels in four directions (Haralick et al., 1973). GLCM has been used in the past to assess surface roughness based on laser speckle images (Lu et al., 2006). It was found and discussed in Ulanowski et al. (2014) that among the four features of the GLCM (contrast, correlation, ~~energy and homogeneity~~ homogeneity and energy, also known as uniformity or angular second moment), energy is the parameter which has the strongest correlation to roughness but is also less biased by external factors (e.g. image brightness change due to camera gain change). Statistical
25 measures describing image brightness distribution are obtained by two methods, firstly by calculating the ratio of root-mean-squared brightness to its standard deviation (RMS/SD) (Jolic et al., 1994) and secondly by calculating the kurtosis of the brightness distribution. This leads to a “combined roughness” measure, following equation:

$$0.7 - \frac{2E}{3} - \frac{(\log K)}{6} + \frac{RMS}{4000SD}, \quad (1)$$

where ~~E~~ E is the energy derived from the GLCM and ~~K~~ K the kurtosis. ~~This~~ The combined measure is dependent on the
30 number of independent “scattering centres” present on the surface of the crystal, so it reflects the overall complexity of ice crystals, including both small-scale roughness as well as larger-scale structure, such as that found in so-called “polycrystals”

(Ulanowski et al., 2012, 2014). The combined roughness has been tested on ice analogues and mineral dust with various surfaces and results that are reported in Ulanowski et al. (2014) show that it does provide a good estimation of a particle surface irregularity. In addition, the size of the ice particles, which is inversely proportional to the average area of speckle spots, is retrieved and is used throughout the present work to determine crystal size. The size measured in this way represents
5 the diameter of equal area circle projected along the line parallel to the laser beam (Ulanowski et al., 2012).

Time-lapse videos showing the evolution of LISA 2-D scattering patterns during cyclic ice growth experiments are shown in the supplementary material (~~video~~-S1 and S2). Broadly, the size of the speckle spots visible in the patterns is a reflection of ice crystal size (strictly speaking its inverse), and the amount of speckle represents crystal roughness. In the videos, growth periods are characterized by the spots shrinking and generally moving inwards, and the opposite occurs during sublimation periods.
10 The presence of isolated bright spots or bands is an indication of flat crystal facets, while spots covering a large proportion of the pattern signify the presence of roughness or high complexity.

3 Results and ~~Discussion~~discussion

In the following, ~~first~~-experiments are presented and discussed first, addressing two aspects; ~~the influences~~: the influence of supersaturation, and of regrowth cycles on the ice crystal surface roughness measures. However, we note that in general
15 other factors may also influence crystal morphology, like the type, shape and size of the INP, the mode of ice nucleation (homogeneous, immersion freezing or deposition nucleation), temperature and ventilation (as represented by the fall speed). For example, the AIDA experiments mentioned above also indicate that homogeneous nucleation ~~leads~~can lead to crystals with strongly rough surfaces (Schnaiter et al., 2016). Furthermore, it has been shown that droplets freezing at lower temperatures are more likely to grow into complex “polycrystals” (Pitter and Pruppacher, 1973; Bacon et al., 2003). Since homogeneous
20 nucleation occurs, by definition, at low temperatures it may lead to the formation of more imperfect crystals; however, we must note that the temperature effect may be secondary to the influence of the high saturation ratios that are necessary to initiate homogeneous nucleation. Investigation of the influence of these parameters is beyond the scope of this paper, but might be addressed in future work.

Fig. 6 shows examples of ~~a smooth and rough~~-2-D scattering patterns ~~of~~from smooth and rough ice columns to illustrate
25 what patterns could be classified as originating from smooth or rough ice crystals in the following discussion. It can be seen that the main characteristic of a rough particle/crystal is the speckle captured by the CCD camera, which is the outcome of complex interference between scattered waves originating from multiple regions of the particle (Ulanowski et al., 2012). Smooth crystals on the other hand do not produce strong speckle, as scattering is dominated by fewer, distinct interactions with the particle, which tend not to produce the interference giving rise to speckle patterns; these interactions are more akin to the reflections
30 and refractions of classical geometric optics but enhanced by diffraction, which leads to the appearance of arc-like features in the 2-D patterns (Clarke et al., 2006). More examples obtained from ice analogues and other types of smooth and rough or irregular particles can be seen in Ulanowski et al. (2014).

Most of the noise visible in the retrieved crystal size and roughness measure in the experiment time series has been found to originate from the gas flow of the laminar flow tube which creates vibrations of the fibre. Slight vibrations of the sample result in scattered data points. However, in all the cases, the trend is discernible and becomes clearer after applying locally weighted scatterplot smoothing (LOESS, Cleveland and Devlin (1988)) to the data points in order to obtain a trend curve for each experiment.

3.1 Slow and fast growth

Fast crystal growth tends to lead to the emergence of roughness on crystal surfaces. Regular, smooth crystals can be grown at low supersaturation, where the growth rate is slow enough for the deposited molecules to diffuse on facets to well-separated attachment sites at steps, kinks, and ledges. In contrast, fast growth promotes attachment anywhere on crystal surface, resulting in roughness. Fast growth can moreover lead to the creation of defects and ionization, which further promote irregular growth (Dash et al., 2001; Dash and Wettlaufer, 2003; Pantarakis and Flood, 2005; Ferreira et al., 2008; Flood, 2010)(Beckmann, 1982; Dash et al., 2001). Supersaturation was identified as one of the main parameters controlling the surface roughness in experiments conducted for ice by Hallett (1987), and complex polycrystals tend to dominate ice habits at high supersaturations (Bacon et al., 2003; Bailey and Hallett, 2004). There is evidence from recent, dedicated experiments in the AIDA cloud chamber that increasing the maximum supersaturation achieved during chamber expansions leads to increased roughness, as indicated by SID-3 measurements (Schnaiter et al., 2016).

Since the supersaturation controls the growth rate but could not be determined ~~precisely~~ directly with high accuracy in our experiments, several slow and fast ice crystal growths experiments at -40°C were performed. Thereby, slow ice crystal growth could be observed at low, and faster growth at higher supersaturation. For comparability, the shape of the investigated ice crystals was kept similar, hence very high supersaturation ratios resulting in the formation of complex ice crystals were excluded, and only single columns were considered. This means that even in the fast growth experiments the supersaturation wrt. ice was less than about 20% (typically between 10 and 20%). The slow growth experiments were done ~~eloseer~~ closer to saturated conditions (typically about 5% supersaturation wrt. ice).

Fig. 7 shows the growth of two regrown ice crystals exposed to different level of supersaturation at -35°C . Based on the flow rate ratio, which was varied between 0.7/4.3 l/min (wet/dry, slow) and 1.0/4.0 l/min (fast), the difference in relative humidity wrt. ice was about 10 percent (compare Fig 5). The crystals can be compared directly as they grow from $20\ \mu\text{m}$ to $29\ \mu\text{m}$, after fitting trend curves using LOESS. The crystal regrown at a higher saturation ratio shows a greater and steeper roughness increase – from 0.27 to 0.39 over 23 seconds, an increase of 0.12, as compared to the crystal exposed to lower humidity – from 0.29 to 0.37 over 100 seconds, an increase of 0.08. In Fig. 8 the relationship between the temporal rate of change of roughness and the growth rate is depicted for ice crystals in the size range from $20\ \mu\text{m}$ to $80\ \mu\text{m}$. Fifteen different growth experiments leading to the formation of simple columns were performed to investigate this relationship with twelve cases where the initial crystal was sublimated and regrown. The correlation was found to be strong, with the coefficient of determination R^2 of 0.82, implying that higher degree of supersaturation leads to faster roughness evolution, i.e. quicker formation of more irregular ice surfaces.

Concerning possible mechanisms for the emergence of roughness during crystal growth, while the general ones discussed above are likely to play a role, an additional one may be important specifically for water ice. Laboratory experiments indicate that ice at atmospherically relevant temperatures, rather than being formed purely from the hexagonal crystallographic phase, can contain numerous stacking faults, where adjacent molecular layers are stacked in the cubic instead of hexagonal sequence, leading to “stacking-disordered ice”. Such structure is associated with the lower symmetry, trigonal crystallographic space group P3m1 (Hansen et al., 2008; Murray et al., 2015) and can lead to the production of scalene ice crystals (Kuhs et al., 2012; Murray et al., 2015). Stacking disorder has been associated with the presence of macroscopic kinks and roughness on prismatic facets (Kuhs et al., 2012). It can occur even at both cold and warmer temperatures (Malkin et al., 2012, 2015). While stacking-disordered ice tends to anneal to hexagonal ice at higher temperatures (Kuhs et al., 2012), its presence in the early stages of growth may nevertheless influence crystal shape, even if the phase is absent from “mature”, crystals. However, we must note that on the basis of molecular modelling the stacking-disordered phase may be less likely to form during growth from vapour than during freezing (Hudait and Molinero, 2016).

3.2 Roughness due to humidity cycles

Another process that could influence the roughness of ice crystals is the exposure to several depositional growth and sublimation cycles (Nelson, 1998; Korolev et al., 1999), which can occur in the atmosphere (Nelson, 1998; Korolev et al., 1999; Ulanowski et al., 2014). Fig. 9 shows an example of how such repeated cycles performed at -30°C can lead to roughness in an initially smooth column. After the initial growth, the saturation ratio with respect to ice was between about 1.0 and 1.05 (based on flow rate ratio, which was set to values between 0.8 l/min and 1.0 l/min wet flow, and 4.2 l/min and 4.0 l/min dry flow, see Fig. 5) and was decreased in order to partly sublimate the crystal. At $t = 140$ s, it can be seen that the column has shrunk and shows a relatively smooth surface with a combined roughness value of about 0.3. The corresponding 2-D scattering pattern is also typical of a relatively smooth column, as can be seen by comparison with Fig. 6. Upon re-growing the crystal, irregularities started forming on the surface, as can be observed in the microscopy image and in the increase of the combined roughness at $t = 250$ s. The ice crystal then was shrunk and regrown again, ending with a combined roughness of about 0.6. A video showing the evolution of the LISA 2-D scattering patterns during the experiment in Fig. 9 is shown in the supplementary material (video-S1). The 10 minute period is condensed into one minute, but the time displayed corresponds to the abscissa in Fig. 9. In the video, the inward and outward drift drifting of speckle spots corresponds to crystal growth and sublimation, respectively.

A second example is shown in Fig. 10. In this experiment an illite particle on the tip of the glass fibre nucleated an ice crystal at a lower temperature of -40°C . The saturation ratio with respect to ice was similar and between about 1.0 and 1.1 (after the initial growth, values based on flow rate ratio, which was set to values between 0.6 l/min and 0.8 l/min wet flow, and 4.4 l/min and 4.2 l/min dry flow, see Fig. 5). A video showing the evolution of the 2-D patterns during the experiment in Fig. 10 is shown in the supplementary material (video-S2); as in the previous video the time is speeded up by a factor of 10. As in Fig. 9, rougher features appear during the second growth cycle, but then also in the additional third cycle. Although more experiments would be required to get robust statistics, these observations indicate that the more growth-sublimation cycles are performed, the rougher the crystal can become. The increase observed in the final roughness appeared to be the outcome of an asymmetric,

irreversible character of the cyclic growth process, i.e. the increase in roughness during a growth phase was not mirrored by an equal decrease of roughness during the subsequent sublimation phase. Thus, the overall outcome was a gradual “ratcheting up” of roughness.

We note that similar behaviour has been postulated by Nelson (1998) who stated that due to asymmetry between the growth and sublimation processes, primarily because of different energy barriers to step formation - weaker in the case of sublimation - repeated growth-sublimation cycles would lead to progressively more complex ice crystals. Furthermore, in experiments carried out under atmospherically-relevant air pressures, crystals having undergone more than one growth cycle tended to develop more faults (Beckmann, 1982). Korolev et al. (1999) stated that cycling of growth and sublimation caused by mixing and small scale vertical motions might be a possible meehanism-route for the formation of irregular crystals. This conjecture is supported by our experiments. It was also suggested by the same authors that “sublimation may cause numerous irregularities on the surface of the ice crystal”. However, while sublimation can in some cases lead to increased roughness, as demonstrated by experiments carried out in Scanning Electron Microscopy (SEM) chambers (Cross, 1969; Pfalzgraff et al., 2010; Neshyba et al., 2013; Ulanowski et al., 2014; Magee et al., 2014), the cyclic growth described here tended to result in a slight reduction in roughness during each sublimation phase.

The apparent disparity between our observations and SEM experiments can be accounted for by the fact that growth in the absence of air that takes place in a SEM chamber, instead of being diffusion-limited-limited by vapour diffusion as is the case for ice at tropospheric pressures, becomes limited by the attachment kinetics (Libbrecht, 2017). This distinction is known to lead to different growth rates as well as habits (Beckmann, 1982; Kuroda and Gonda, 1984; Libbrecht, 2017). Consequently, during SEM observations water molecule removal can take place anywhere on facet surfaces, leading to pronounced roughness. Moreover, the bunching of elementary molecular steps, possibly due to the Schwoebel effect (Misbah et al., 2010), can result in the creation of larger, microscopic (as opposed to elementary) steps that can be seen in SEM micrographs (Cross, 1969). In contrast, in the diffusion-limited regime sublimation tends to remove material near crystal edges and vertices, which can lead to reduced roughness (and rounding), as was the case in our observations. However, for very small crystals the relative impact of diffusion is diminished anyway (Yokoyama and Kuroda, 1990), so we conjecture that sublimation of such crystals might potentially lead to increased roughness even at tropospheric pressures.

A further difference between the diffusion limited and kinetics-limited growth is that the former can lead to increased numbers of faults (Beckmann, 1982) and dendritic, skeletal, or needle-shaped crystals, while the latter tends to produce more perfect, smooth, isometric prisms (Gonda, 1976, 1977) – with similarity to the SEM chamber experiments. Thus stronger departure from smooth, regular crystal shapes – roughness in a general sense - can be expected at tropospheric pressures, provided that the crystals are large enough compared to the mean free path of the water molecule at the given pressure (Yokoyama and Kuroda, 1990).

Another feature of the growth process may be borne out by the cyclic growth experiments. Careful examination of the retrieved crystal size shown in Fig 9 indicates markedly slower growth in later cycles, despite similar supersaturation levels. A similar effect was in the past observed for crystallization from solution - a reduction of the growth rate of sucrose crystals that previously experienced a period of rapid growth (Pantaraks and Flood, 2005; Ferreira et al., 2008; Flood, 2010). Thus

a “memory effect” may be present, which not only leads to increased roughness in subsequent growth cycles but ~~–~~results in reduced growth rates under identical supersaturations. This reduction can at first sight be contrary to expectations: high roughness, reflected by high density of surface defects, might lead to increased growth rate under kinetically-limited growth conditions. However, this would not occur when growth is diffusion limited, as is the case at tropospherically relevant air pressures. On the contrary, defects resulting from fast growth may inhibit the incorporation of molecules on the crystal surface, possibly through the introduction of impurities (Ferreira et al., 2008; Flood, 2010). Nevertheless we caution that this potentially very important finding must be confirmed through carefully controlled experiments, to eliminate the possibility that the reduced growth rate may have been caused by instrumental factors, such as a reduction of supersaturation in later cycles.

3.3 Atmospheric ~~Implications~~implications

It is important to mention that certain atmospheric parameters cannot be reproduced in the current experimental setup. These parameters, like air pressure (Neshyba et al., 2013), radiative heating/cooling or fall velocity can potentially influence the shape of the crystals and their complexity (Hallett, 1987). For example, ice crystal growth is significantly influenced by the ventilation effect (Westbrook and Heymsfield, 2011); high velocities favour plate-like over dendritic habits (Keller and Hallett, 1982); roughness can emerge at lower supersaturations for falling crystals than for stationary ones (Yokoyama and Kuroda, 1990). As stated above, the flow velocity in IRIS is about 1 m/s, which is slightly higher than the typical fall velocity of ice crystals in the atmosphere; consequently, at more atmospherically relevant velocities, crystal roughness might conceivably become greater than observed here. Airflow could also create asymmetry of the ice crystal shape (Takahashi and Mori, 2006) and therefore the same crystal can have quite different properties depending on its orientation.

Nevertheless, the combined roughness values obtained in the experiments shown here during the two re-growth cycles (values between 0.55 and 0.65) are comparable to the values encountered in mid-latitude cirrus and mixed-phase clouds during CONSTRAIN (Ulanowski et al., 2014), indicating that the results are at least qualitatively comparable.

Very high supersaturation regions can be encountered in clean air at cirrus altitudes or within cirrus clouds. Several studies reported supersaturations with respect to ice up to 140% (the onset of homogeneous ice nucleation) within a temperature range from -33°C to -73°C (Gierens et al., 1999, 2000; Ovarlez et al., 2002; Spichtinger et al., 2003, 2004; Krämer et al., 2009). It is very likely, as shown in our experiments, that at higher supersaturation rougher crystals ~~will develop at the expense~~ tend to develop instead of smoother ones. The low temperatures at which homogeneous nucleation becomes dominant may be an additional factor leading to increased crystal roughness in the broad sense, as droplets freezing at lower temperatures are more likely to grow into complex “polycrystals” (Pitter and Pruppacher, 1973; Bacon et al., 2003). On the other hand, high number concentrations of homogeneously nucleated ice lead to quick depletion of available water vapour, hence the ice growth rate can be expected to rapidly peak and then decline. We suggest that disentangling these conflicting influences may be possible through cloud chamber studies.

Humidity variation is omnipresent in cirrus. For example, Kübbeler et al. (2011) and Krämer et al. (2009) show that saturation with respect to ice can depart widely from equilibrium. Therefore, mixing and small scale vertical motions in clouds, leading to the presence of many depositional growth and sublimation regions, may be a possible mechanism by which roughness emerges

(Korolev et al., 1999). In both cirrus and mixed phase clouds, high-resolution modelling predicts that ice particle trajectories can contain multiple super- and subsaturated regions (Flossmann and Wobrock, 2010; Kübbeler et al., 2011). Such inhomogeneity can be seen as arising from temperature fluctuations due to turbulence at various scales or gravity waves. Indeed, agreement between models and cirrus ice measurements is improved by the inclusion of such fluctuations, in comparisons across a broad
5 range of geographical latitudes (Hoyle et al., 2005; Engel et al., 2013; Jensen et al., 2013). Provided that the ice crystals do not fully sublimate following such cyclic growth, this process would lead to creating rougher ice crystals. Moreover, longer-lived (older) clouds may contain higher incidence and/or intensity of roughness than short-lived ones. The history of individual ice crystals may also impact their subsequent growth rates, as discussed in section 3.2. Therefore future microphysical or parameterized cloud models may be improved by the introduction of such a memory effect, in addition to temperature and
10 humidity.

Finally, we note that rough ice surfaces are associated with stronger electrical charging (Caranti and Illingworth, 1983; Dash et al., 2001; Dash and Wettlaufer, 2003), hence the presence of roughness may influence storm electrification. If so, measures of roughness based on 2-D scattering patterns could be an indicator of the cloud electrification potential of ice crystals, since they are sensitive to the presence of multiple scattering centres on ice surfaces, corresponding to the unevenness of the surfaces.

15 **4 Conclusions and outlook**

An experimental system was developed to investigate light scattering properties of single ice crystals grown on a glass fibre in dependence on the prevailing thermodynamic conditions. The system, called Ice Roughness Investigation System (IRIS), is based on the laminar flow tube LACIS and a laboratory version of the Small Ice Detector 3 (SID-3), which was additionally equipped with an optical microscope. The thermodynamic conditions during the experiments are controlled by varying the dry
20 and wet gas flows passing through the flow tube, allowing changes of temperature and saturation ratio over a wide range on a time scale of less than 5 s.

First investigations of the impact of the saturation ratio and cyclic growth on the development of ice crystal roughness show that repeated depositional growth-sublimation cycles lead to progressively increasing ice crystal roughness, as indicated by 2-D scattering patterns. Results also show that the higher the supersaturation, the faster the increase in roughness. Moreover,
25 crystal growth rate appears to be lower later in the cycles, once roughness has developed, hinting at an additional memory effect.

Further experiments should be performed to achieve a better understanding of the influence of supersaturation on the development of rough ice crystals at different temperatures. In addition, it is also of high importance to investigate what is the impact of the nature of the ice nucleating particle and the nucleation mechanism on the development of roughness. In particular,
30 cloud chamber experiments should elucidate the influence of the dynamics of the homogeneous nucleation process, whereby large initial supersaturation leading potentially to increased roughness (due to fast growth) may be counteracted by reduced supersaturation due to the presence of high ice crystal concentrations (i.e. slow growth). Experiments comparing the degree of roughness from repeated humidity cycles with different frequencies (i.e. the same growth and sublimation rates (i.e. humidity

amplitude) and total duration but shorter or longer cycles) would elucidate whether the lifetime of the cloud or the frequency of fluctuations is more important for roughness development. Finally, the sensitivity of ice crystal growth rate to growth history, in particular the resulting roughness, should be investigated, with a view to improving future cloud models. Such improvements may allow more accurate representation of not just roughness but crystal size too, and hence characteristics such as radiative properties, cloud lifetime, precipitation development, and possibly also cloud electrification properties.

Author contributions: C.C., J.V., P.H., H.B. designed and carried out the experiments including sample preparation and data analysis with assistance from T.C. J.V. performed the computational fluid dynamics simulations. Z.U. conceived and supervised the project and provided crystal property measurement techniques and interpretation of ice growth processes. F.S., Z.U., J.V. developed the main conceptual ideas and the technical details of the experiments and the experimental setup IRIS. C.C., J.V., Z.U. wrote the manuscript with support from P.H., H.B., F.S, T.C., D.N., S.H. and G.R. All authors discussed the results.

Competing interests: The authors declare that they have no conflict of interest.

Supplementary material related to this article is available online at: [doi:10.5446/35425](https://doi.org/10.5446/35425) (video S1) and [doi:10.5446/35426](https://doi.org/10.5446/35426) (video S2)

Acknowledgements: This work was supported by the UK Natural Environment Research Council grant NE/I020067/1 (ACID-PRUF) and the EU Eurochamp-2 scheme grant E2-2011-12-06-0065. The concept of LISA was proposed by Alexei Kiselev, and the instrument itself was designed and built by Edwin Hirst at the University of Hertfordshire. We also acknowledge Christabel Tan for preparing the chemical solution used to clean the fibres.

References

- Auriol, F., Gayet, J.-F., Febvre, G., Jourdan, O., Labonnote, L., and Brogniez, G.: In situ observations of cirrus cloud scattering phase function with 22° and 46° halos: Cloud field study on 19 February 1998, *J. Atmos. Sci.*, 58, 3376–3390, doi:10.1175/1520-0469(2001)058<3376:ISOOCS>2.0.CO;2, 2001.
- 5 Bacon, N. J., Baker, M. B., and Swanson, B. D.: Initial stages in the morphological evolution of vapour-grown ice crystals: A laboratory investigation, *Q. J. Roy. Meteor. Soc.*, 129, 1903–1927, doi:10.1256/qj.02.04, 2003.
- Bailey, M. and Hallett, J.: Growth rates and habits of ice crystals between -20° and -70°C, *J. Atmos. Sci.*, 61, 514–544, doi:10.1175/1520-0469(2004)061<0514:GRAHOI>2.0.CO;2, 2004.
- Baran, A. J.: From the single-scattering properties of ice crystals to climate prediction: A way forward, *Atmos. Res.*, 112, 45–69, doi:10.1016/j.atmosres.2012.04.010, 2012.
- Baumgardner, D., Abel, S. J., Axisa, D., Cotton, R., Crosier, J., Field, P., Gurganus, C., Heymsfield, A., Korolev, A., Kraemer, M., et al. Lawson, P., McFarquhar, G., Ulanowski, Z., and Um, J.: Cloud ice properties: in situ measurement challenges, *Meteor. Monographs*, 58, 9–19, 1–9, 23, doi:10.1175/AMSMONOGRAPHS-D-16-0011.1, 2017.
- Beckmann, W.: [Interface kinetics of the growth and evaporation of ice single crystals from the vapour phase: III. Measurements under partial pressures of nitrogen](#), *J. Cryst. Growth*, 58, 443–451, doi:10.1016/0022-0248(82)90291-3, 1982.
- 15 Boucher, O., Randall, D., Artaxo, P., Bretherton, C., Feingold, G., Forster, P., Kerminen, V.-M., Kondo, Y., Liao, H., Lohmann, U., et al.: Clouds and aerosols, in: *Climate change 2013: the physical science basis. Contribution of Working Group I to the Fifth Assessment Report of the Intergovernmental Panel on Climate Change*, pp. 571–657, Cambridge University Press, <https://doi.org/doi:10.1017/CBO9781107415324.016>, 2013.
- 20 Caranti, J. M. and Illingworth, A. J.: The contact potential of rimed ice, *J. Phys. Chem.*, 87, 4125–4130, doi:10.1021/j100244a028, 1983.
- Clarke, A. J. M., Hesse, E., Ulanowski, Z., and Kaye, P. H.: A 3D implementation of ray tracing combined with diffraction on facets: Verification and a potential application, *J. Quant. Spectrosc. Ra. trans.*, 100, 103–114, doi:10.1016/j.jqsrt.2005.11.028, 2006.
- Cleveland, W. S. and Devlin, S. J.: Locally weighted regression: an approach to regression analysis by local fitting, *J. Am. Stat. Assoc.*, 83, 596–610, doi:10.1080/01621459.1988.10478639, 1988.
- 25 Connolly, P. J., Flynn, M. J., Ulanowski, Z., Choularton, T. W., Gallagher, M. W., and Bower, K. N.: Calibration of 2-D imaging probes using calibration beads and ice crystal analogues, *J. Atmos. Ocean. Tech.*, 24, 1860–1879, doi:10.1175/JTECH2096.1, 2007.
- Cotton, R., Osborne, S., Ulanowski, Z., Hirst, E., Kaye, P. H., and Greenaway, R.: The ability of the Small Ice Detector (SID-2) to characterize cloud particle and aerosol morphologies obtained during flights of the FAAM BAe-146 research aircraft, *J. Atmos. Ocean. Tech.*, 27, 290–303, doi:10.1175/2009JTECHA1282.1, 2010.
- 30 Cross, J. D.: Scanning electron microscopy of evaporating ice, *Science*, 164, 174–175, doi:10.1126/science.164.3876.174, 1969.
- Dash, J. G. and Wettlaufer, J. S.: The surface physics of ice in thunderstorms, *Canadian J. Phys.*, 81, 201–207, doi:10.1139/p03-011, 2003.
- Dash, J. G., Mason, B. L., and Wettlaufer, J. S.: Theory of charge and mass transfer in ice-ice collisions, *J. Geophys. Res.*, 106, 20 395–20 402, doi:10.1029/2001JD900109, 2001.
- Dymarska, M., Murray, B. J., Sun, L., Eastwood, M. L., Knopf, D. A., and Bertram, A. K.: Deposition ice nucleation on soot at temperatures relevant for the lower troposphere, *J. Geophys. Res.*, 111, [D04 204](#), doi:10.1029/2005JD006627, 2006.
- 35

- Engel, I., Luo, B. [P.](#), Pitts, M. [C.](#), Poole, L. [R.](#), Hoyle, C. [R.](#), Grooß, J.-U., Dörnbrack, A., and Peter, T.: Heterogeneous formation of polar stratospheric clouds—Part 2: Nucleation of ice on synoptic scales, *Atmos. Chem. Phys.*, 13, 10769–10785, doi:10.5194/acp-13-10769-2013, 2013.
- Ferreira, A., Faria, N., and Rocha, F.: Roughness effect on the overall growth rate of sucrose crystals, *J. Cryst. Growth*, 310, 442–451, doi:10.1016/j.jcrysgro.2007.11.031, 2008.
- Field, P. [R.](#), Heymsfield, A. [J.](#), and Bansemmer, A.: Shattering and particle interarrival times measured by optical array probes in ice clouds, *J. Atmos. Ocean. Tech.*, 23, 1357–1371, doi:10.1175/JTECH1922.1, 2006.
- Flood, A. E.: Feedback between crystal growth rates and surface roughness, *Cryst. Eng. Comm.*, 12, 313–323, doi:10.1039/B914913A, 2010.
- Flossmann, A. I. and Wobrock, W.: A review of our understanding of the aerosol–cloud interaction from the perspective of a bin resolved cloud scale modelling, *Atmos. Res.*, 97, 478–497, doi:10.1016/j.atmosres.2010.05.008, 2010.
- Foot, J. S.: Some observations of the optical properties of clouds. II: Cirrus, *Q. J. Royal Meteorol. Soc.*, 114, 145–164, doi:10.1002/qj.49711447908, 1988.
- Garrett, T. J., Hobbs, P. V., and Gerber, H.: Shortwave, single-scattering properties of arctic ice clouds, *J. Geophys. Res.*, 106, 15 155–15 172, doi:10.1029/2000JD900195, 2001.
- 15 Gierens, K., Schumann, U., Helten, M., Smit, H., and Marenco, A.: A distribution law for relative humidity in the upper troposphere and lower stratosphere derived from three years of MOZAIC measurements, *Ann. Geophys.*, 17, 1218–1226, doi:10.1007/s00585-999-1218-7, 1999.
- Gierens, K., Schumann, U., Helten, M., Smit, H., and Wang, P.-H.: Ice-supersaturated regions and subvisible cirrus in the northern midlatitude upper troposphere, *J. Geophys. Res.*, 105, 22 743–22 753, doi:10.1029/2000JD900341, 2000.
- 20 Gonda, T.: The growth of small ice crystals in gases of high and low pressures, *J. Meteor. Soc. Japan*, 54, 233–240, doi:10.2151/jmsj1965.54.4_233, 1976.
- Gonda, T.: The growth of small ice crystals in gases of high and low pressures at -30 and -44°C, *J. Meteor. Soc. Japan*, 55, 142–146, doi:10.2151/jmsj1965.55.1_142, 1977.
- Hallett, J.: Faceted snow crystals, *J. Opt. Soc. Am.*, 4, 581–588, doi:10.1364/JOSAA.4.000581, 1987.
- 25 Hansen, T. [C.](#), Koza, M. [M.](#), and Kuhs, W. [F.](#): Formation and annealing of cubic ice: I. Modelling of stacking faults, *J. Phys.*, 20, 285 104, doi:10.1088/0953-8984/20/28/285104, 2008.
- Haralick, R. M., Shanmugam, K., ~~et al~~ [and Dinstein, I.](#): Textural features for image classification, *IEEE T. Syst. Man. Cyb.*, pp-[SMC-3](#), 610–621, <https://doi.org/10.1109/TSMC.1973.4309314>, 1973.
- Hartmann, D. L., Ockert-Bell, M. E., and Michelsen, M. L.: The effect of cloud type on Earth’s energy balance: Global analysis, *J. Clim.*, 5, 1281–1304, doi:10.1175/1520-0442(1992)005<1281:TEOCTO>2.0.CO;2, 1992.
- 30 Hartmann, S., Niedermeier, D., Voigtländer, J., Clauss, T., Shaw, R. [A.](#), Wex, H., Kiselev, A., and Stratmann, F.: Homogeneous and heterogeneous ice nucleation at LACIS: operating principle and theoretical studies, *Atmos. Chem. Phys.*, 11, 1753–1767, doi:10.5194/acp-11-1753-2011, 2011.
- Heymsfield, A. J., Krämer, M., Luebke, A., Brown, P., Cziczo, D. J., Franklin, C., Lawson, P., Lohmann, U., McFarquhar, G., Ulanowski, Z., ~~et al~~ [and VanTricht, K.](#): Cirrus clouds, *Meteor. Monographs*, 58, [2,1–2.26](#), doi:10.1175/AMSMONOGRAPHS-D-16-0010.1, 2017.
- Hioki, S., Yang, P., Baum, B. A., Platnick, S., Meyer, K. G., King, M. D., and Riedi, J.: Degree of ice particle surface roughness inferred from polarimetric observations, *Atmos. Chem. Phys.*, 16, 7545–7558, doi:10.5194/acp-16-7545-2016, 2016.

- Hoyle, C. [R.](#), Luo, B. [P.](#), and Peter, T.: The origin of high ice crystal number densities in cirrus clouds, *J. Atmos. Sci.*, 62, 2568–2579, doi:10.1175/JAS3487.1, 2005.
- Hudait, A. and Molinero, V.: What determines the ice polymorph in clouds?, *J. Amer. Chem. Soc.*, 138, 8958–8967, doi:10.1021/jacs.6b05227, 2016.
- 5 Jensen, E. [J.](#), Lawson, P., Baker, B., Pilson, B., Mo, Q., Heymsfield, A. [J.](#), Bansemer, A., Bui, T. [P.](#), McGill, M., Hlavka, D., et al.: On the importance of small ice crystals in tropical anvil cirrus, *Atmos. Chem. Phys.*, 9, 5519–5537, doi:10.5194/acp-9-5519-2009, 2009.
- Jensen, E. [J.](#), Lawson, R. [P.](#), Bergman, J. [W.](#), Pfister, L., Bui, T. [P.](#), and Schmitt, C. [G.](#): Physical processes controlling ice concentrations in synoptically forced, midlatitude cirrus, *J. Geophys. Res.*, 118, 5348–5360, doi:10.1002/jgrd.50421, 2013.
- Jolic, K. [I.](#), Nagarajah, C. [R.](#), and Thompson, W.: Non-contact, optically based measurement of surface roughness of ceramics, *Meas. Sci. Technol.*, 5, 671–684, doi:10.1088/0957-0233/5/6/007, 1994.
- 10 Kaye, P. H., Hirst, E., Greenaway, R. S., Ulanowski, Z., Hesse, E., DeMott, P. J., Saunders, C., and Connolly, P.: Classifying atmospheric ice crystals by spatial light scattering, *Opt. Lett.*, 33, 1545–1547, doi:10.1364/OL.33.001545, 2008.
- Keller, V. [W.](#) and Hallett, J.: Influence of air velocity on the habit of ice crystal growth from the vapor, *J. Crystal Growth*, 60, 91–106, doi:10.1016/0022-0248(82)90176-2, 1982.
- 15 Korolev, A. [V.](#), Isaac, G. [A.](#), and Hallett, J.: Ice particle habits in Arctic clouds, *Geophys. Res. Lett.*, 26, 1299–1302, doi:10.1029/1999GL900232, 1999.
- Korolev, A. [V.](#), Emery, E. [F.](#), Strapp, J. [W.](#), Cober, S. [G.](#), Isaac, G. [A.](#), Wasey, M., and Marcotte, D.: Small ice particles in tropospheric clouds: Fact or artifact? Airborne Icing Instrumentation Evaluation Experiment, *Bull. Amer. Meteor. Soc.*, 92, 967–973, doi:10.1175/2010BAMS3141.1, 2011.
- 20 Krämer, M., Schiller, C., Afchine, A., Bauer, R., Gensch, I., Mangold, A., Schlicht, S., Spelten, N., Sitnikov, N., Borrmann, S., deReus, M., and Spichtinger, P.: Ice supersaturations and cirrus cloud crystal numbers, *Atmos. Chem. Phys.*, 9, 3505–3522, doi:10.5194/acp-9-3505-2009, 2009.
- Kübbeler, M., Hildebrandt, M., Meyer, J., Schiller, C., Hamburger, T., Jurkat, T., Minikin, A., Petzold, A., Rautenhaus, M., Schlager, H., Schumann, U., Voigt, C., Spichtinger, P., Gayet, J., Gourbeyre, C., and Krämer, M.: Thin and subvisible cirrus and contrails in a subsaturated environment, *Atmos. Chem. Phys.*, 11, 5853–5865, doi:10.5194/acp-11-5853-2011, 2011.
- 25 Kuhs, W. F., Sippel, C., Falenty, A., and Hansen, T. C.: Extent and relevance of stacking disorder in "ice Ic", *Proc. Natl. Acad. Sci.*, 109, 21 259–21 264, doi:10.1073/pnas.1210331110, 2012.
- [Kuroda, T. and Gonda, T.: Rate determining processes of growth of ice crystals from the vapour phase, Part II: investigations of surface kinetic processes, *J. Meteor. Soc. Jap.*, 62, 563–572, doi:10.2151/jmsj1965.62.3_563, 1984.](#)
- 30 Libbrecht, K. G.: Physical ~~Dynamics of Ice Crystal Growth~~[dynamics of ice crystal growth](#), *Annu. Rev. Mat. Res.*, 47, 271–295, doi:10.1146/annurev-matsci-070616-124135, 2017.
- Liu, C., Panetta, R. L., and Yang, P.: The effects of surface roughness on the scattering properties of hexagonal columns with sizes from the Rayleigh to the geometric optics regimes, *J. Quant. Spectrosc. Radiat. Transf.*, 129, 169–185, doi:10.1016/j.jqsrt.2013.06.011, 2013.
- Lu, R.-S., Tian, G.-Y., Gledhill, D., and Ward, S.: Grinding surface roughness measurement based on the co-occurrence matrix of speckle pattern texture, *Appl. Opt.*, 45, 8839–8847, doi:10.1364/AO.45.008839, 2006.
- 35 Magee, N. [B.](#), Miller, A., Amaral, M., and Cumiskey, A.: Mesoscopic surface roughness of ice crystals pervasive across a wide range of ice crystal conditions, *Atmos. Chem. Phys.*, 14, 12357–12371, doi:10.5194/acp-14-12357-2014, 2014.

- Malkin, T. L., Murray, B. J., Brukhno, A. V., Anwar, J., and Salzmann, C. G.: Structure of ice crystallized from supercooled water, *Proc. Natl. Acad. Sci.*, 109, 1041–1045, doi:10.1073/pnas.1113059109, 2012.
- Malkin, T. L., Murray, B. J., Salzmann, C. G., Molinero, V., Pickering, S. J., and Whale, T. F.: Stacking disorder in ice I, *Phys. Chem. Chem. Phys.*, 17, 60–76, doi:10.1039/C4CP02893G, 2015.
- 5 McFarquhar, G. M. and Heymsfield, A. J.: Parameterization of tropical cirrus ice crystal size distributions and implications for radiative transfer: Results from CEPEX, *J. Atmos. Sci.*, 54, 2187–2200, doi:10.1175/1520-0469(1997)054<2187:POTCIC>2.0.CO;2, 1997.
- McFarquhar, G. M., Heymsfield, A. J., Spinhirne, J., and Hart, B.: Thin and subvisual tropopause tropical cirrus: Observations and radiative impacts, *J. Atmos. Sci.*, 57, 1841–1853, doi:10.1175/1520-0469(2000)057<1841:TASTTC>2.0.CO;2, 2000.
- [Misbah, C., Pierre-Louis, O., and Saito, Y.: Crystal surfaces in and out of equilibrium: A modern view, *Rev. Mod. Phys.*, 82, 981–1040, doi:10.1103/RevModPhys.82.981, 2010.](#)
- 10 Murray, B. J., Salzmann, C. G., Heymsfield, A. J., Dobbie, S., Neely III, R. R., and Cox, C. J.: Trigonal ice crystals in Earth’s atmosphere, *Bull. Amer. Meteor. Soc.*, 96, 1519–1531, doi:10.1175/BAMS-D-13-00128.1, 2015.
- Nelson, J.: Sublimation of ice crystals, *J. Atmos. Sci.*, 55, 910–919, doi:10.1175/1520-0469(1998)055<0910:SOIC>2.0.CO;2, 1998.
- Neshyba, S. [P.](#), Lowen, B., Benning, M., Lawson, A., and Rowe, P. [M.](#): Roughness metrics of prismatic facets of ice, *J. Geophys. Res.*, 118, 3309–3318, doi:10.1002/jgrd.50357, 2013.
- 15 Ovarlez, J., Gayet, J.-F., Gierens, K., Ström, J., Ovarlez, H., Auriol, F., Busen, R., and Schumann, U.: Water vapour measurements inside cirrus clouds in Northern and Southern hemispheres during INCA, *Geophys. Res. Lett.*, 29, [60–1–60–4](#), doi:10.1029/2001GL014440, 2002.
- Pantaraks, P. and Flood, A. E.: Effect of growth rate history on current crystal growth: A second look at surface effects on crystal growth rates, *Cryst. Growth Des.*, 5, 365–371, doi:10.1021/cg049863k, 2005.
- Pfzgraff, W. [C.](#), Hulscher, R. [M.](#), and Neshyba, S. [P.](#): Scanning electron microscopy and molecular dynamics of surfaces of growing and ablating hexagonal ice crystals, *Atmos. Chem. Phys.*, 10, 2927–2935, doi:10.5194/acp-10-2927-2010, 2010.
- Pitter, R. [L.](#) and Pruppacher, H. [R.](#): A wind tunnel investigation of freezing of small water drops falling at terminal velocity in air, *Q. J. Roy. Meteor. Soc.*, 99, 540–550, doi:10.1002/qj.49709942111, 1973.
- 25 Sassen, K., Wang, Z., and Liu, D.: Cirrus clouds and deep convection in the tropics: Insights from CALIPSO and CloudSat, *J. Geophys. Res.*, 114, [D00H06](#), doi:10.1029/2009JD011916, 2009.
- Schmitt, C. G., Schnaiter, M., Heymsfield, A. J., Yang, P., Hirst, E., and Bansemmer, A.: The Microphysical Properties of Small Ice Particles Measured by the Small Ice Detector-3 Probe during the MACPEX Field Campaign, *J. Atmos. Sci.*, 73, 4775–4791, doi:10.1175/JAS-D-16-0126.1, 2016.
- 30 Schnaiter, M., Järvinen, E., Vochezer, P., Abdelmonem, A., Wagner, R., Jourdan, O., Mioche, G., Shcherbakov, V., Schmitt, C., Tricoli, U., [et al](#) [Ulanowski, Z., and Heymsfield, A. J.](#): Cloud chamber experiments on the origin of ice crystal surface roughness in cirrus clouds, *Atmos. Chem. Phys.*, [16, 5091–5110](#), doi:10.5194/acp-16-5091-2016, [2015–2016](#).
- Spichtinger, P., Gierens, K., and Read, W.: The global distribution of ice-supersaturated regions as seen by the Microwave Limb Sounder, *Q. J. Roy. Meteor. Soc.*, 129, 3391–3410, doi:10.1256/qj.02.141, 2003.
- 35 Spichtinger, P., Gierens, K., Smit, H. [G. J.](#), Ovarlez, J., and Gayet, J.-F.: On the distribution of relative humidity in cirrus clouds, *Atmos. Chem. Phys.*, 4, 639–647, doi:10.5194/acp-4-639-2004, 2004.

- Stratmann, F., Kiselev, A., Wurzler, S., Wendisch, M., Heintzenberg, J., Charlson, R. [J.](#), Diehl, K., Wex, H., and Schmidt, S.: Laboratory studies and numerical simulations of cloud droplet formation under realistic supersaturation conditions, *J. Atmos. Ocean. Technol.*, 21, 876–887, doi:10.1175/1520-0426(2004)021<0876:LSANSO>2.0.CO;2, 2004.
- Takahashi, C. and Mori, M.: Growth of snow crystals from frozen water droplets, *Atmos. Res.*, 82, 385–390, doi:10.1016/j.atmosres.2005.12.013, 2006.
- Ulanowski, Z., Hesse, E., Kaye, P. H., Baran, A. J., and Chandrasekhar, R.: Scattering of light from atmospheric ice analogues, *J. Quant. Spectrosc. Ra.*, 79, 1091–1102, doi:10.1016/S0022-4073(02)00342-4, 2003.
- Ulanowski, Z., Connolly, P., Flynn, M., Gallagher, M., Clarke, A. [J. M.](#), and Hesse, E.: Using ice crystal analogues to validate cloud ice parameter retrievals from the CPI ice spectrometer data, *Proc. 14 Int. Conf. Clouds and Precip.*, pp. 1175–1178, <http://hdl.handle.net/2299/6753>, 2004.
- Ulanowski, Z., Hesse, E., Kaye, P. H., and Baran, A. J.: Light scattering by complex ice-analogue crystals, *J. Quant. Spectrosc. Ra.*, 100, 382–392, doi:10.1016/j.jqsrt.2005.11.052, 2006.
- Ulanowski, Z., Hirst, E., Kaye, P. H., and Greenaway, R.: Retrieving the size of particles with rough and complex surfaces from two-dimensional scattering patterns, *J. Quant. Spectrosc. Ra.*, 113, 2457–2464, doi:10.1016/j.jqsrt.2012.06.019, 2012.
- Ulanowski, Z., Kaye, P. H., Hirst, E., Greenaway, R. [S.](#), Cotton, R. J., Hesse, E., and Collier, C. T.: Incidence of rough and irregular atmospheric ice particles from Small Ice Detector 3 measurements, *Atmos. Chem. Phys.*, 14, 1649–1662, doi:10.5194/acp-14-1649-2014, 2014.
- Voigtländer, J., Stratmann, F., Niedermeier, D., Wex, H., and Kiselev, A.: Mass accommodation coefficient of water: A combined computational fluid dynamics and experimental data analysis, *J. Geophys. Res.*, 112, [D20 208](#), doi:10.1029/2007JD008604, 2007.
- Westbrook, C. D. and Heymsfield, A. J.: Ice crystals growing from vapor in supercooled clouds between -2.5°C and -22°C: Testing current parameterization methods using laboratory data, *J. Atmos. Sci.*, 68, 2416–2429, doi:10.1175/JAS-D-11-017.1, 2011.
- Wylie, D., Jackson, D. L., Menzel, W. P., and Bates, J. J.: Trends in global cloud cover in two decades of HIRS observations, *J. Climate*, 18, 3021–3031, doi:10.1175/JCLI3461.1, 2005.
- Yang, P., Hong, G., Kattawar, G. W., Minnis, P., and Hu, Y.: Uncertainties associated with the surface texture of ice particles in satellite-based retrieval of cirrus clouds – Part II: Effect of particle surface roughness on retrieved cloud optical thickness and effective particle size, *IEEE Trans. Geosci. Remote Sens.*, 46, 1948–1957, doi:10.1109/TGRS.2008.916472, 2008a.
- Yang, P., Kattawar, G. W., Hong, G., Minnis, P., and Hu, Y.: Uncertainties associated with the surface texture of ice particles in satellite-based retrieval of cirrus clouds – Part I: Single-scattering properties of ice crystals with surface roughness, *IEEE Trans. Geosci. Remote Sens.*, 46, 1940–1947, doi:10.1109/TGRS.2008.916471, 2008b.
- Yang, P., Liou, K.-N., Bi, L., Liu, C., Yi, B., and Baum, B. A.: On the radiative properties of ice clouds: Light scattering, remote sensing, and radiation parameterization, *Adv. Atmos. Sci.*, 32, 32–63, doi:10.1007/s00376-014-0011-z, 2015.
- Yi, B., Yang, P., Baum, B. A., L’Ecuyer, T., Oreopoulos, L., Mlawer, E. J., Heymsfield, A. J., and Liou, K.-N.: Influence of ice particle surface roughening on the global cloud radiative effect, *J. Atmos. Sci.*, 70, 2794–2807, doi:10.1175/JAS-D-13-020.1, 2013.
- Yokoyama, E. and Kuroda, T.: Pattern formation in growth of snow crystals occurring in the surface kinetic process and the diffusion process, *Phys. Rev. A*, 41, [2038](#)[2038–2050](#), doi:10.1103/PhysRevA.41.2038, 1990.

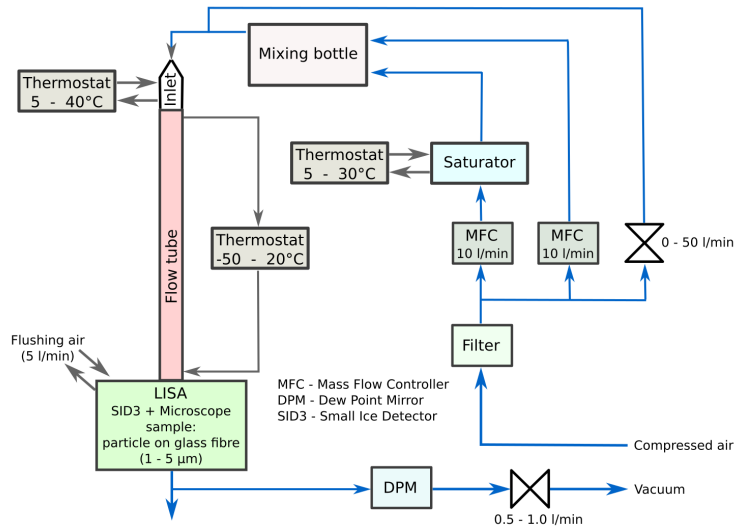


Figure 1. Simplified schematic of the Ice Roughness Investigation System (IRIS).

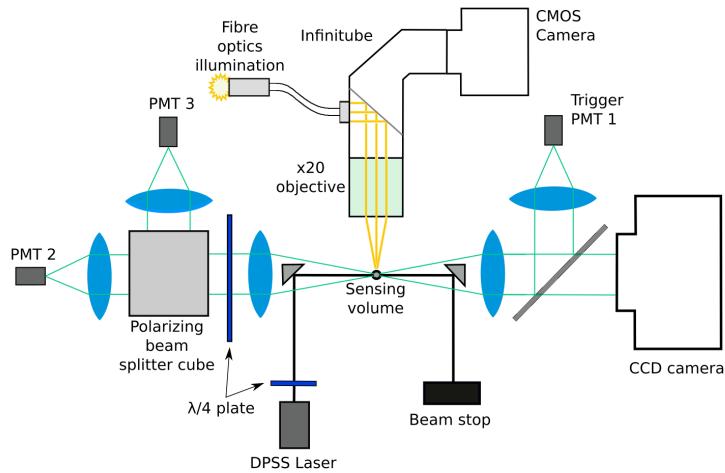
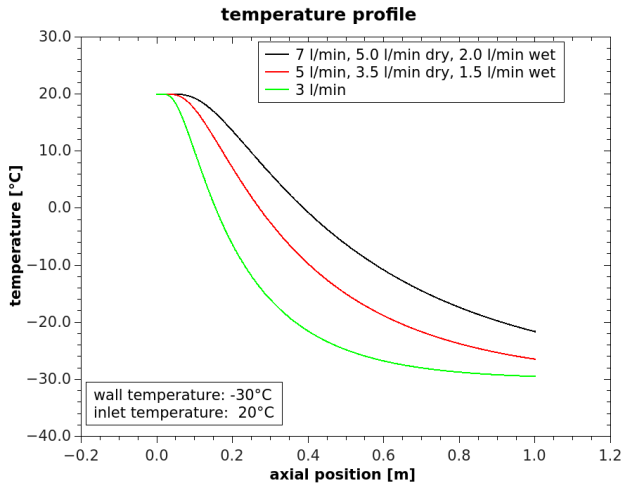
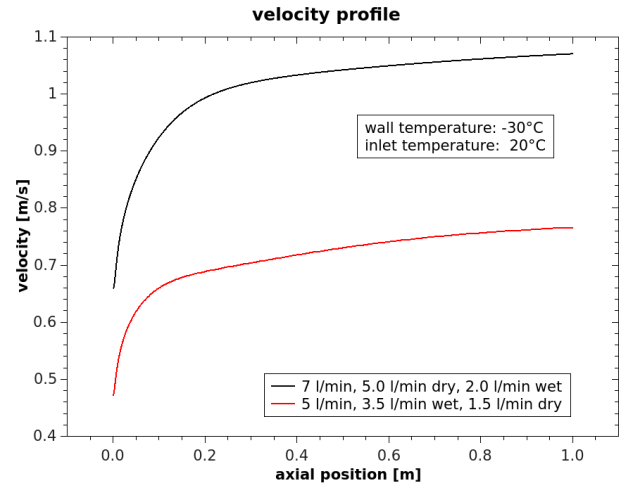


Figure 2. Schematic of the Leipzig Ice Scattering Apparatus (LISA), the optical system of IRIS.

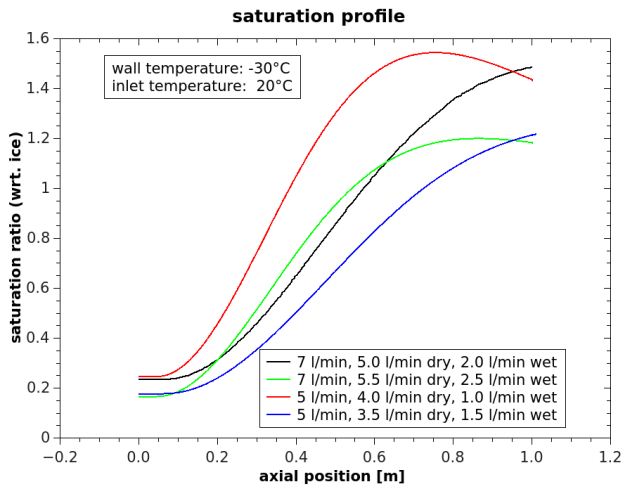
Measured temperatures in the observation volume of LISA. Measuring points are represented by the black dots and the coloured contours are interpolated values.



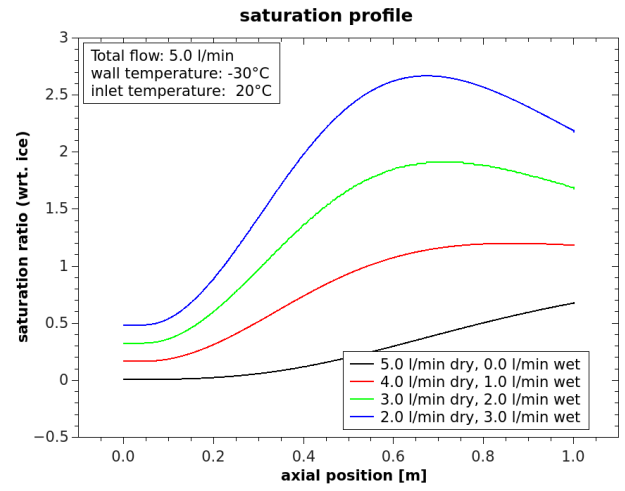
(a)



(b)



(c)



(d)

Figure 3. Examples of calculated flow velocity (a), temperature (b) and saturation ratio (bottom) profiles along the tube axis. The simulations were done with the CFD code Fluent. The tube length in the simulations was 1.2m, while it is only 1.0m in the experimental setup.

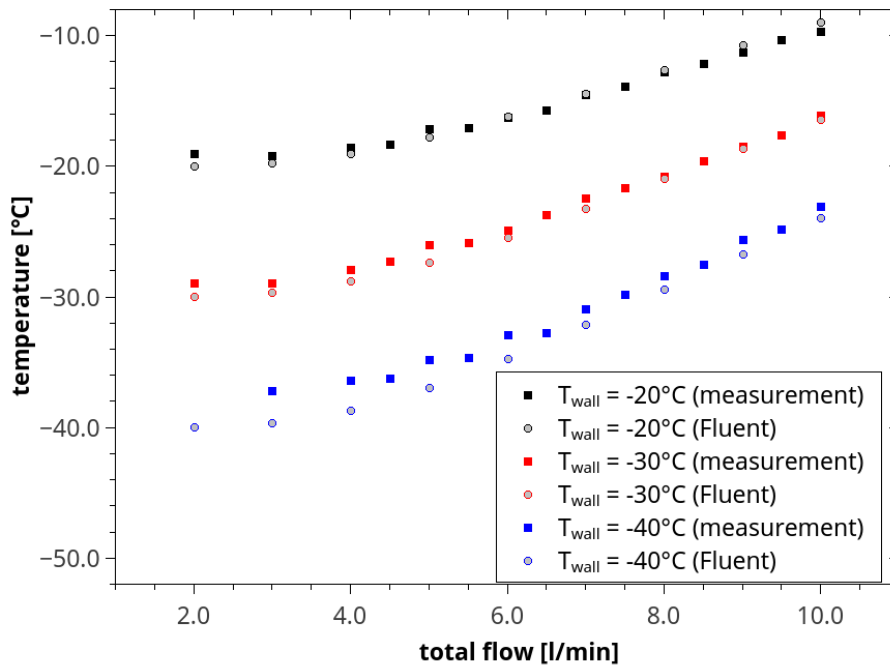


Figure 4. Comparison between measured and calculated temperature in dependence of the total flow rate using three different wall temperatures. [The solid lines represent interpolation of the experimental data.](#)

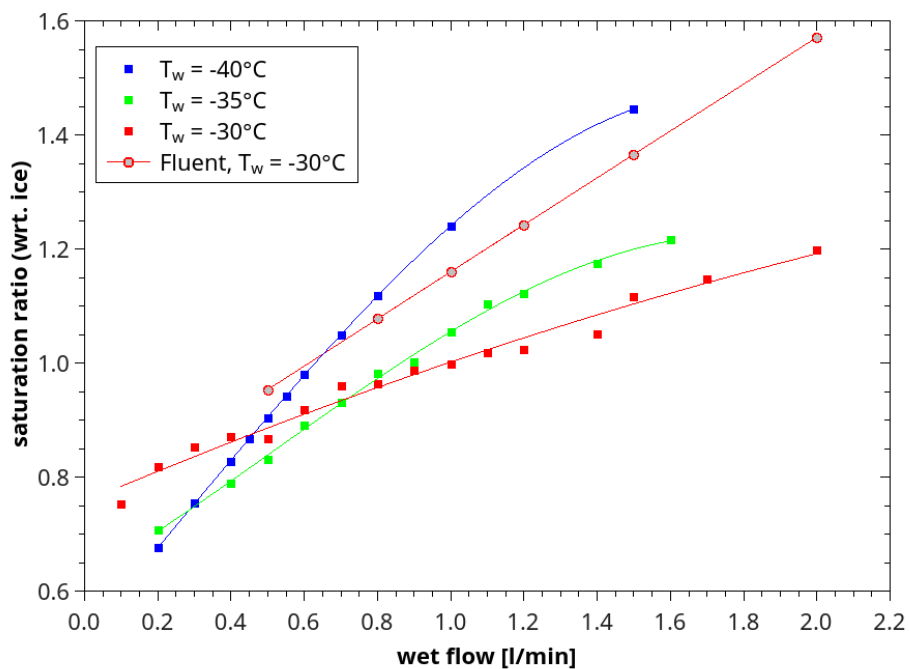


Figure 5. Measured (circles) and modelled (squares) relative humidity (wrt. ice) in the sampling volume of LISA. Measured temperatures in the observation volume of LISA. The total flow rate was 5 l/min. The values are given in dependence of the wet flow rate.

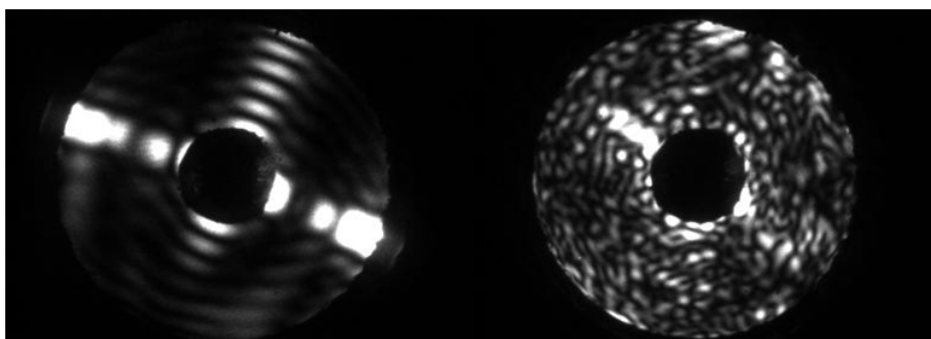


Figure 6. 2-D scattering [pattern-patterns](#) of a smooth column (left panel) and a rough column (right panel). [The patterns were produced using the SID3 instrument in the AIDA cloud chamber during growth at low \(left\) and high \(right\) supersaturation \(Schnaiter et al., 2016\).](#)

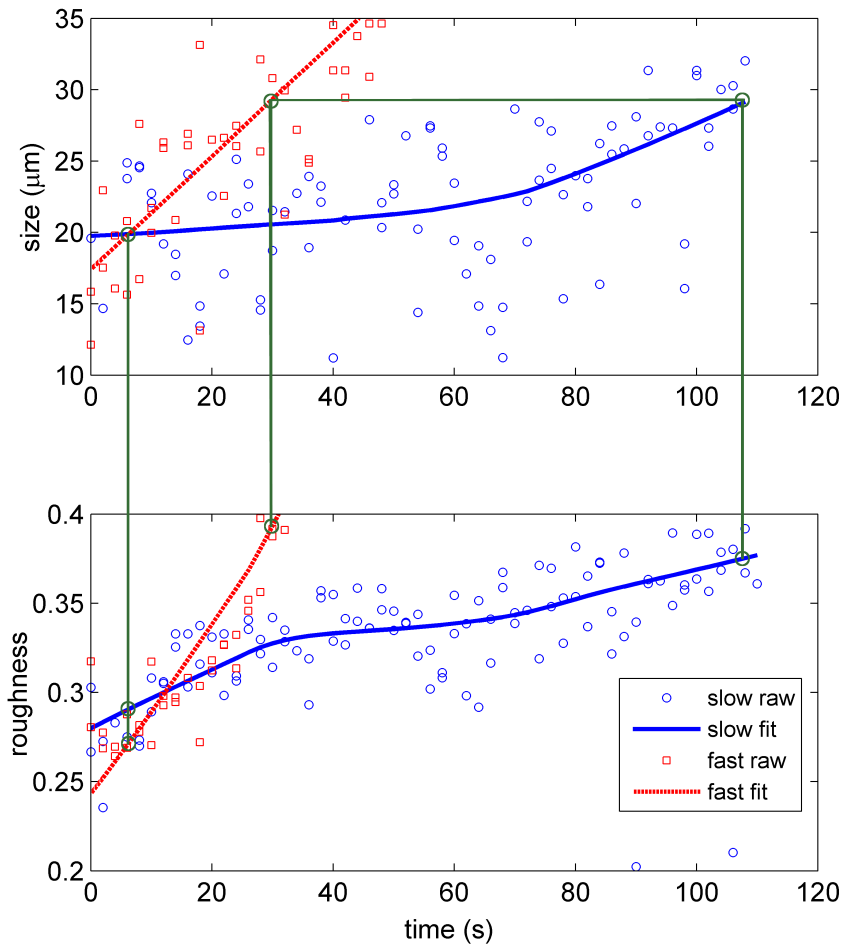


Figure 7. Size and roughness of two pre-existing ice crystals exposed to different supersaturations (difference about 10 percent): slow growth (blue symbols and lines) and fast growth (red symbol and lines); the trend curves were fitted using LOESS. The crystals can be compared directly as they grow from $20\ \mu\text{m}$ to $29\ \mu\text{m}$. Based on the flow rate ratio, which was varied between 0.7/4.3 l/min (wet/dry, slow) and 1.0/4.0 l/min (fast), the difference in relative humidity wrt. ice was about 10 percent (compare Fig 5).

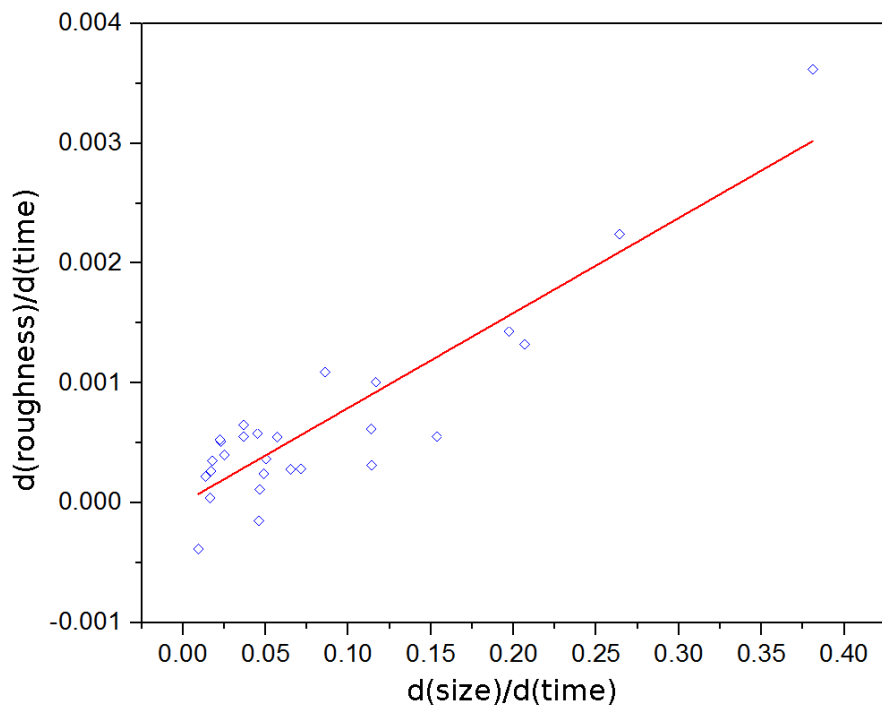


Figure 8. Rate of increase of roughness as a function of the growth rate (indicating the degree of supersaturation in the flow tube). Each point corresponds to a separate growth experiment. The coefficient of determination R^2 is 0.82.

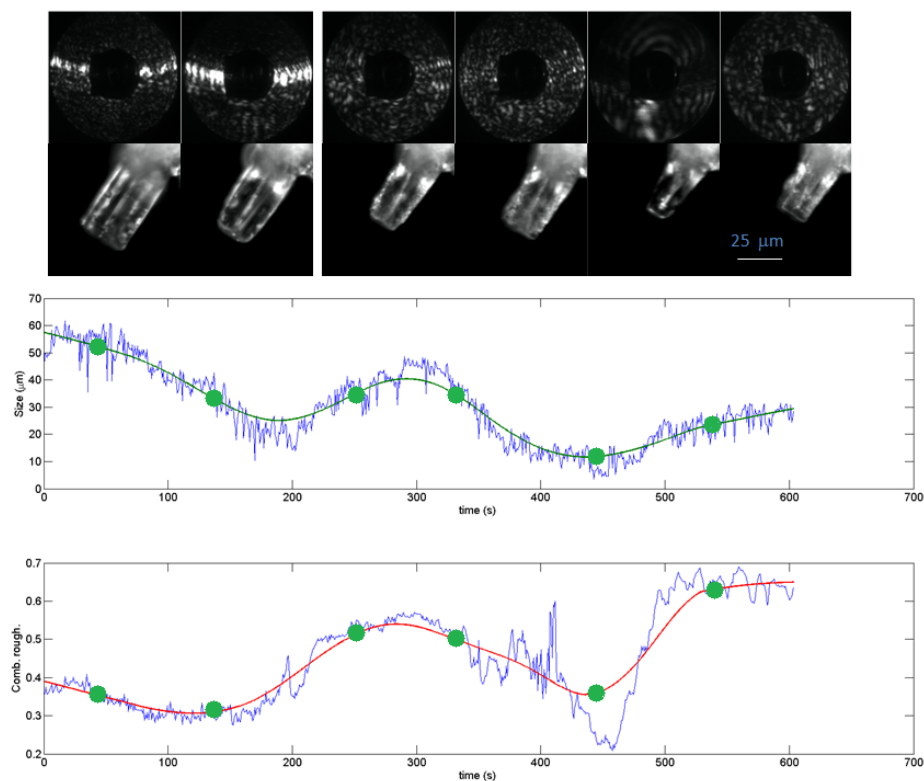


Figure 9. Cyclic growth-sublimation experiments with a single ice prism nucleated on a glass fibre at -30°C . After the initial growth, the saturation ratio with respect to ice was between about 1.0 and 1.05 (based on flow rate ratio, which was set to values between 0.8 l/min and 1.0 l/min wet flow, and 4.2 l/min and 4.0 l/min dry flow, see Fig. 5) and was decreased in order to partly sublimate the crystal. First row shows the 2-D scattering patterns with the corresponding time marked in green. Second row shows the ice crystal at the indicated times. The blue curves below show the actual retrieved data for particle size and roughness. The corresponding green and red best-fit curves were obtained using LOESS regression. A time-lapse video showing the entire sequence of LISA 2-D patterns is given in the supplemental material ([video S1](#)), labelled with experiment time.

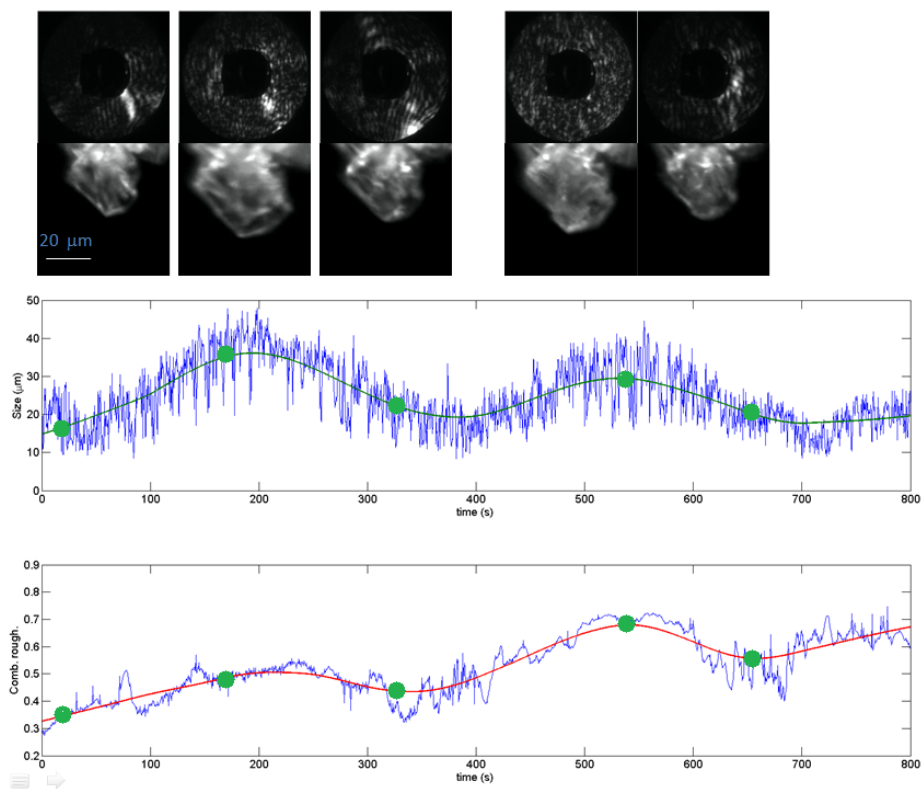


Figure 10. As Fig. 9 but for an ice crystal nucleated on an illite particle at -40°C . A video showing the 2-D patterns is given in the supplemental material ([video-S2](#)).

Supplement S3 S4 S5

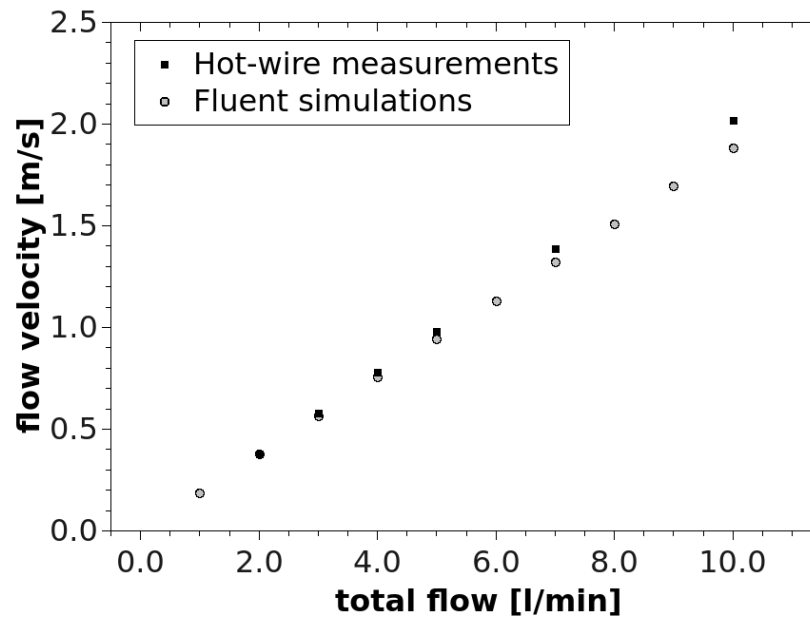


Figure S3: Measured and simulated velocity at the center outlet of the laminar flow diffusion chamber with respect to the total flow. The measurements were done by means of an hot-wire anemometer (Dantec Dynamics, Denmark). The miniature hot-wire sensor (Dantec 55P11 sensor) was fixed at the tube outlet in the measuring volume of the laser beam. Single point measurements were done in dependence of the total flow. The data were compared to Fluent simulation results. Both, measurements and simulations were done at 20° and dry conditions.

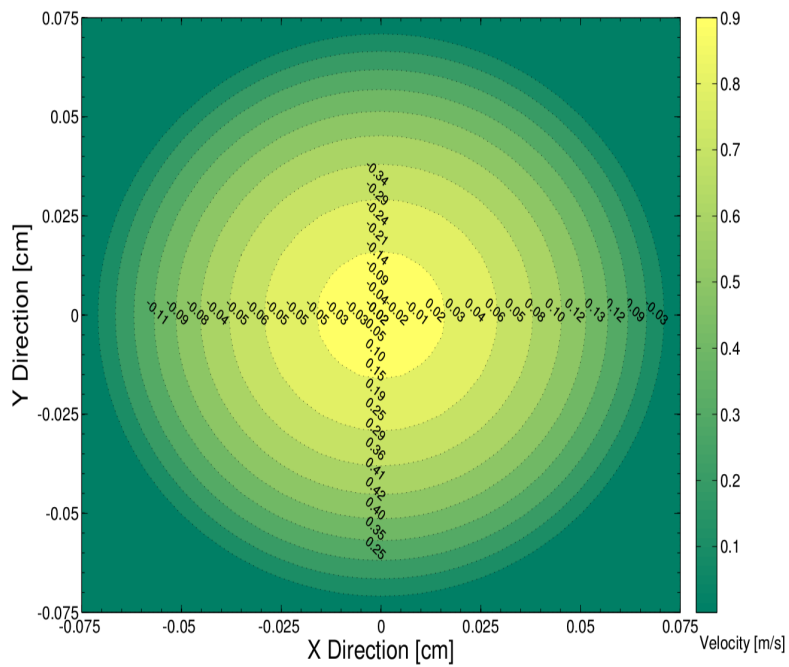


Figure S4: Illustration of calculated velocity data (contour plot of Fluent simulation results) and the difference between measurements and calculations (values). The position of the numbers corresponds to the measurement position of the hot-wire sensor in the cross sectional profile at the tube outlet.

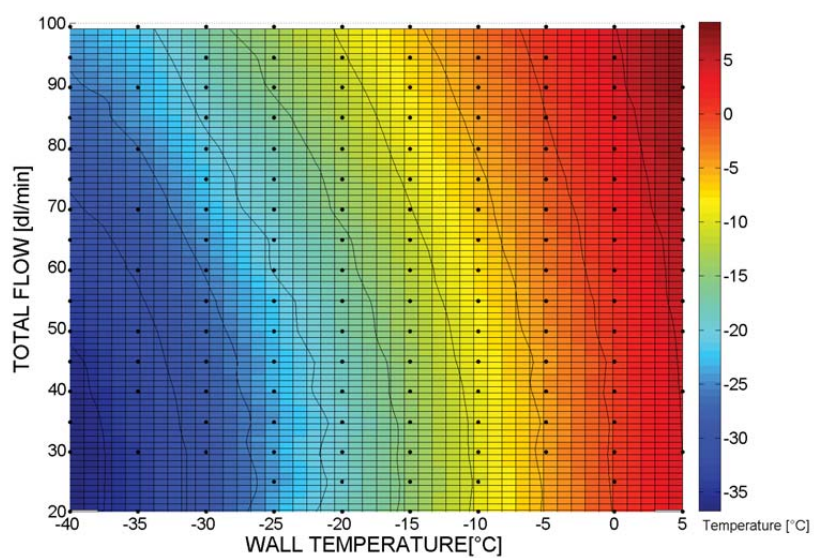


Figure S5: Contour plot of the temperature characterization results. The figure was obtained by a linear interpolation of the temperature measurements (black dots). the black lines are temperature isolines. The figure illustrates that IRIS can be used over a broad temperature range.